

GRAFS: Graph Analytics Fusion and Synthesis

FARZIN HOUSHMAND, University of California, Riverside, USA

MOHSEN LESANI, University of California, Riverside, USA

KEVAL VORA, Simon Fraser University, Canada

Graph analytics elicits insights from large graphs to inform critical decisions for business, safety and security. Several large-scale graph processing frameworks feature efficient runtime systems; however, they often provide programming models that are low-level and subtly different from each other. Therefore, end users can find implementation and specially optimization of graph analytics time-consuming and error-prone. This paper regards the abstract interface of the graph processing frameworks as the instruction set for graph analytics, and presents GRAFS, a high-level declarative specification language for graph analytics and a synthesizer that automatically generates efficient code for five high-performance graph processing frameworks. It features novel semantics-preserving fusion transformations that optimize the specifications and reduce them to three primitives: reduction over paths, mapping over vertices and reduction over vertices. Reductions over paths are commonly calculated based on push or pull models that iteratively apply kernel functions at the vertices. This paper presents conditions, parametric in terms of the kernel functions, for the correctness and termination of the iterative models, and uses these conditions as specifications to automatically synthesize the kernel functions. Experimental results show that the generated code matches or outperforms hand-optimized code, and that fusion accelerates execution.

1 INTRODUCTION

Large-scale *graph analytics* has recently gained popularity due to its growing applicability across various important domains including social networks, market influencer analysis, bioinformatics, criminology, and machine learning and data mining. Several large-scale graph processing systems [Gonzalez et al. 2012; Malewicz et al. 2010; Roy et al. 2013; Shun and Blelloch 2013; Zhang et al. 2018; Zhu et al. 2016, 2015] have been developed to enable efficient graph analysis across shared memory and distributed platforms. The provided programming models require graph analysis problems to be expressed in terms of local kernel functions over vertices and edges. However, graph analyses are best expressed using *higher-level abstractions* such as reduction over paths. For instance, shortest path, reachability and connected component problems are fundamentally formulated in terms of paths. Further, elaborate graph analysis problems that involve multiple reductions over paths or vertices are difficult to correctly implement using the offered low-level programming models. More importantly, manual *optimizations* such as merging multiple iterations can be time-consuming and error-prone. In particular, reasoning about the *correctness and termination* properties requires challenging analysis on the values of vertices across iterations that emulate values for paths.

This project regards the interface of the graph processing frameworks as the instruction set for graph analytics, and introduces GRAFS, a graph analytics language and synthesizer. The GRAFS language is a *high-level declarative specification language* that provides features for common graph processing idioms such as reduction over paths, and mapping and reduction over vertices. We show that it can easily and concisely capture the common graph analysis problems. Given a specification, the GRAFS synthesizer *automatically synthesizes code* for five graph processing frameworks: Ligra [Shun and Blelloch 2013], GridGraph [Zhu et al. 2015], PowerGraph [Gonzalez et al. 2012], Gemini [Zhu et al. 2016], and GraphIt [Zhang et al. 2018].

To synthesize efficient implementations, GRAFS optimizes the specification by syntactic *fusion transformations* that fuse similar operations to be executed together. We formalize the syntax and the semantics of the GRAFS language and the fusion rules, and prove that fusion is semantics-preserving. As described above, fusion reduces specifications to the sequence of three primitives: reduction over paths, mapping over vertices and reduction over vertices.

Graph analytics frameworks offer *iterative programming models* to calculate reduction over paths. The values for vertices or edges are calculated iteratively based on the values of neighbors. Influenced by their runtime systems, these frameworks differ on how values are propagated between iterations. For example, PowerGraph [Gonzalez et al. 2012] allows computations to pull in values from incoming neighbors or to push out values to outgoing neighbors, whereas Ligra [Shun and Blueloch 2013] and GridGraph [Zhu et al. 2015] only allow pushing values. Further, Gemini [Zhu et al. 2016] requires both pull-based and push-based implementations of the computation so that it can dynamically switch between the two to maximize performance. Not only the propagation methods, but also *system-specific* nuances make the implementation of the same analysis problem subtly different from a framework to another. For example, a push-based implementation in Ligra requires an atomic function that operates over a single edge whereas Gemini requires two functions: the first determines the value to be pushed from the source, and the second operates directly over the outgoing edges, and updates the target values atomically.

We formalize several *iteration models* that given certain kernel functions, calculate path-based reductions. For each iteration model, we present *correctness and termination conditions* for candidate kernel functions. Given a path-based reduction, GRAFS synthesizer enumerates candidate kernel functions and uses the correctness conditions as specifications to automatically *synthesize the kernel functions*. Fusion reduces specifications to reduction over paths, mapping over vertices and reduction over vertices. Subsequently, the synthesizer reduces path-based reductions to iterative calculations. Thus, graph analysis is reduced to *iteration-map-reduce primitives*. We show how each of these primitives can be immediately implemented in each of the five target frameworks.

We apply GRAFS to common graph analysis use-cases and generate code for each of the five frameworks. The experimental results show that synthesized programs are equally or more efficient than hand-optimized programs, and that fusion significantly reduces execution time.

In summary, this paper makes the following contributions: (1) The graph analytics specification language GRAFS and its semantics (§ 2 and § 4.1), (2) Semantics-preserving and platform-independent fusion transformations to optimize graph analytics (§ 4.2), (3) The formalization of iterative graph computation models (§ 3), their correctness and termination conditions (§ 5.1), and synthesis of their kernel functions (§ 5.2), and (4) The GRAFS synthesis tool that generates code for five graph processing frameworks and its experimental results (§ 6).

2 OVERVIEW

We start with an overview. We first present the GRAFS specification language through examples, and then show how specifications can be fused to equivalent more efficient specifications. Then, we illustrate iterative reductions and present a glimpse of their correctness conditions and how the kernel functions can be synthesized.

Graph Analysis Specification. The GRAFS language declaratively and concisely captures *mathematical specifications of graph analysis computations*. The language design is guided by common idioms in graph processing use-cases. GRAFS supports reduction over values of paths to a vertex and also mapping and reduction over values of vertices. We present example specifications in Fig. 1. More use-cases are available in the appendix § 1 [Appendix 2019].

The use-case **SSSP** specifies the weight of the shortest path from the source vertex s to each vertex v . The set of paths from a source vertex s to a destination vertex v is denoted by $\text{Paths}(s, v)$.

The specification applies the minimum reduction function \min to the result of applying the weight function weight to all paths p in $\text{Paths}(s, v)$. The specification of connected component (for undirected graphs) **CC** takes the smallest identifier of the vertices in a component as the representative identifier of that component. The set of all paths (from any source vertex) to a destination vertex v is denoted by $\text{Paths}(v)$. The specification **CC** defines the connected component of each vertex v as the minimum identifier of the head vertices of the paths $\text{Paths}(v)$. The above two specifications apply a reduction function \mathcal{R} to the result of a path function \mathcal{F} for a set of paths. We call these reductions *path-based reductions*. Similarly, the breadth-first-search use-case **BFS** finds the parent of each vertex in the breadth-first-search tree. For each vertex v , it specifies a path-based reduction to find the shortest-length path from the source s to the vertex v and returns the penultimate of that path. The penultimate of a path is the vertex before the last in the path. The specification uses the reduction function $\arg \min$ to get the path with the minimum length rather than the minimum length itself, and then applies the penultimate function to the path. A simpler specification can simply apply \min and return the minimum path length.

Path-based reductions can be nested.

The use-case **WSP** specifies the widest shortest path from a source s to each vertex v . We use the let syntactic sugar to enhance readability. **WSP** has a nested reduction (with the reduction function $\arg \min$) to find the shortest paths, and then a nesting reduction to find the widest capacity in those paths. **WSP** is used as a metric of the trust of a user to other users in social networks where the capacity of each edge is the local trust rating of the source user to the sink user [Golbeck 2005]. Intuitively, users with wider (stronger trust ratings) and shorter (closer) paths are more trustworthy sources of information. Similarly, the use-case **NSP** specifies the number of shortest paths from a source s to each vertex v . It uses a nested reduction to find the shortest paths and then applies the cardinality operator to the resulting set. (We will see in § 4.3 that cardinality is a syntactic sugar for a path-based reduction with the sum \sum function.) Mathematical operators can be applied to path-based reductions. The use-case **NWR** specifies the narrowest to widest path ratio from a source to each vertex. It divides two path-based reductions. Similarly, the use-case **TRUST** is the result of division and maximum operations between path-based reductions. It

$$\begin{aligned}
\text{SSSP}(s)(v) &= \min_{p \in \text{Paths}(s, v)} \text{weight}(p) \\
\text{CC}(v) &= \min_{p \in \text{Paths}(v)} \text{head}(p) \\
\text{BFS}(s)(v) &= \text{penultimate}(\arg \min_{p \in \text{Paths}(s, v)} \text{length}(p)) \\
\text{WSP}(s)(v) &= \text{let } P := \arg \min_{p \in \text{Paths}(s, v)} \text{length}(p) \text{ in} \\
&\quad \max_{p \in P} \text{capacity}(p) \\
\text{NSP}(s)(v) &= \left| \arg \min_{p \in \text{Paths}(s, v)} \text{weight}(p) \right| \\
\text{NWR}(s)(v) &= \frac{\min_{p \in \text{Paths}(s, v)} \text{capacity}(p)}{\max_{p \in \text{Paths}(s, v)} \text{capacity}(p)} \\
\text{TRUST}(v) &= \max_{s \in \bar{s}} \left(\frac{\max_{p \in \text{Paths}(s, v)} \text{capacity}(p)}{\min_{p \in \text{Paths}(s, v)} \text{length}(p)} \right) \\
\text{RADIUS} &= \min_{s \in \{\bar{s}\}} \max_{v \in V} \min_{p \in \text{Paths}(s, v)} \text{length}(p) \\
\text{DRR} &= \frac{\max_{s \in \{\bar{v}\}} \max_{v \in V} \min_{p \in \text{Paths}(s, v)} \text{length}(p)}{\min_{s \in \{\bar{v}\}} \max_{v \in V} \min_{p \in \text{Paths}(s, v)} \text{length}(p)} \\
\text{DS}(s) &= \bigcup_{v \in V \wedge \left(\min_{p \in \text{Paths}(s, v)} \text{weight}(p) \right) > 7} \{v\} \\
\text{RDS}(s) &= \text{let } \text{SSSP} := \lambda s, v. \min_{p \in \text{Paths}(s, v)} \text{weight}(p) \text{ in} \\
&\quad \text{let } \text{WP} := \lambda s, v. \max_{p \in \text{Paths}(s, v)} \text{capacity}(p) \text{ in} \\
&\quad \min_{v \in V \wedge \text{SSSP}(s, v) < \text{RADIUS}} \text{WP}(s, v)
\end{aligned}$$

Fig. 1. A subset of use-cases in GRAFS.

$$\text{RADIUS} = \min_{s \in \{s_1, s_2\}} \max_{v \in V} \min_{p \in \text{Paths}(s, v)} \text{length}(p) \quad (1)$$

$$= \min \left(\max_{v \in V} \min_{p \in \text{Paths}(s_1, v)} \text{length}(p), \max_{v \in V} \min_{p \in \text{Paths}(s_2, v)} \text{length}(p) \right) \quad (2)$$

$$= \min \left(\left(\begin{array}{l} \text{ilet } x := \min_{s_1} \text{ length in} \\ \text{mlet } x' := x \text{ in} \\ \text{rlet } x'' := \max x' \text{ in} \\ x'' \end{array} \right), \left(\begin{array}{l} \text{ilet } y := \min_{s_2} \text{ length in} \\ \text{mlet } y' := y \text{ in} \\ \text{rlet } y'' := \max y' \text{ in} \\ y'' \end{array} \right) \right) \quad (3)$$

$$= \left(\begin{array}{l} \text{ilet } \langle x, y \rangle := \langle \min_{s_1} \text{ length}, \min_{s_2} \text{ length} \rangle \text{ in} \\ \text{mlet } \langle x', y' \rangle := \langle x, y \rangle \text{ in} \\ \text{rlet } \langle x'', y'' \rangle := \langle \max x', \max y' \rangle \text{ in} \\ \min(x'', y'') \end{array} \right) \quad (4)$$

$$= \left(\begin{array}{l} \text{ilet } \langle x, y \rangle := \mathcal{R}_{\langle s_1, s_2 \rangle} \mathcal{F} \text{ in} \\ \text{mlet } \langle x', y' \rangle := \langle x, y \rangle \text{ in} \\ \text{rlet } \langle x'', y'' \rangle := \langle \max x', \max y' \rangle \text{ in} \\ \min(x'', y'') \end{array} \right) \quad \text{where} \quad \begin{array}{l} \mathcal{F} := \lambda p. \langle \text{length}(p), \text{length}(p) \rangle \\ \mathcal{R}(\langle a, b \rangle, \langle a', b' \rangle) := \\ \langle \min(a, a'), \min(b, b') \rangle \end{array} \quad (5)$$

$$= \left(\begin{array}{l} \text{ilet } \langle x, y \rangle := \mathcal{R}_{\langle s_1, s_2 \rangle} \mathcal{F} \text{ in} \\ \text{mlet } \langle x', y' \rangle := \langle x, y \rangle \text{ in} \\ \text{rlet } \langle x'', y'' \rangle := \mathcal{R}' \langle x', y' \rangle \text{ in} \\ \min(x'', y'') \end{array} \right) \quad \text{where} \quad \begin{array}{l} \mathcal{R}'(\langle a, b \rangle, \langle a', b' \rangle) := \\ \langle \max(a, a'), \max(b, b') \rangle \end{array} \quad (6)$$

Fig. 2. Fusion of the **RADIUS** use-case.

specifies the trust from a set of users $\{\bar{s}\}$ to each other user. As before, wider and shorter paths are favored.

The values of vertices calculated by a path-based reduction can be subsequently reduced by a *vertex-based reduction*. The **RADIUS** use-case specifies the radius of the graph by sampling the eccentricity of a set of sources $\{\bar{s}\}$. A vertex-based reduction with the reduction function \max finds the longest of the shortest paths over all vertices. Similar to path-based reductions, mathematical operators can be applied to vertex-based reductions. As the set of sampled sources is finite, the outer \min function can be unrolled to an infix operator between vertex-based reductions. Similarly, the use-case **DRR**, that is the ratio of the the diameter over the radius of the graph, is specified as division, maximum and minimum operations between vertex-based reductions.

The use-case **DS** specifies the set of vertices with the distance of at least 7 from the source s . The union \cup vertex-based reduction is used to calculate the set. The set of vertices that it is applied to are constrained by a nested path-based reduction to specify the distance. (In § 4.3, we show that constrained vertex-based reductions can be desugared to standard vertex-based reductions that are applied to path-based reductions on pairs of values.) Similarly, the use-case **RDS** is specified as a constrained vertex-based reduction. Given a source s , it calculates the narrowest of the widest paths to vertices within the radius of s (k -hop neighbourhood of s where k is the radius of the graph). In a social network, **RDS** can represent a measure of the least amount of trust from a user to her neighbourhood.

Fusion. A naive execution of specifications may execute path-based and vertex-based reductions multiple times. We show that multiple such reductions can be fused into a single reduction and

represented as a common triple-let form with separate terms for path-based reduction, mapping over vertices and vertex-based reduction. The fused computation can execute significantly faster.

For example, the **RADIUS** use-case that we saw in Fig. 1 includes multiple path-based reductions one per source that can be fused together. Further, the path-based reductions are enclosed by vertex-based reductions that can be fused together as well. We illustrate this fusion in Fig. 2. For simplicity, we consider sampling for two sources $\{s_1, s_2\}$. We consider the fusion steps in turn. The specification of **RADIUS** is represented in Eq. 1. In Eq. 2, the outer min function over the two sources is unrolled. In Eq. 3, we restate each of the two reductions in a *triple-let* form. GRAFS features a triple-let term that separates path-based reductions, mapping over vertices and vertex-based reductions, and thus facilitates fusion. The term $\max_{v \in V} \min_{p \in \text{Paths}(s_1, v)} \text{length}(p)$ is rewritten as the following three lets. The first let, $\text{ilet } x := \min_{s_1} \text{length}$, calculates a path-based reduction. For each vertex, it calculates the weight of the shortest path from the source s_1 and binds the result to x . The second let applies a map function on the results of the path-based reductions in each vertex. In this case, there is only one path-based reduction; therefore, the map function in the second let, $\text{mlet } x' := x$, is simply the identity function. (In use-cases that the nesting vertex-based reduction is applied to an expression over path-based reductions, the map in the second let captures the expression.) After fusion, the second let applies division as the map function.) The third let calculates a reduction over all vertices. In this example, $\text{rlet } x'' := \max x'$ calculates the maximum value of over all vertices and binds the result to x'' .

Next, in Eq. 4, the two triple-let terms are fused into one by pairing the operations of the corresponding lets. The outer min is applied to the two final results x'' and y'' . In the next two steps, the paired path-based and vertex-based reductions are fused. In Eq. 5, the two path-based reductions of the first let are fused into one. The two sources s_1 and s_2 are used to initialize the first and second elements of the pairs respectively. The fused reduction calculates the pair of the two values simultaneously. The fused path function \mathcal{F} returns the pair of the results of the two path functions. Similarly, the fused reduction function \mathcal{R} applies the two reduction functions to the first and second elements of the input pairs respectively. Finally, in Eq. 6, the pair of vertex-based reductions of the third let are fused into one. The fused reduction function \mathcal{R}' applies the two reduction functions to the first and second elements of the input pairs respectively. This simple example showcased fusion. We formally present the complete set of fusion rules in § 4.2.

The final term represents the original specification of **RADIUS** as an equivalent sequence of one path-based reduction, one map in each vertex, and one reduction over all vertices. Path-based reduction are calculated iteratively. Thus, fusion reduces GRAFS specifications to three primitives: *Iteration-Map-Reduce*: iteration for iterative path-based reduction, map for mapping over vertices and reduce for reduction over vertices. Map and reduce over vertices can be directly implemented; we now discuss iterative path-based reduction.

Iteration. Calculating path-based reductions by explicit enumeration of paths is prohibitively inefficient. Instead, path-based reductions are calculated iteratively by local updates on the value of vertices based on the values of their neighbors. As an example, we consider the pull model for idempotent reduction functions. Let us consider the simple shortest path use-case **SSSP** that we saw in Fig. 1. It specifies a path-based reduction from the source s where the reduction function \mathcal{R} is min and the path function \mathcal{F} is length.

Each vertex stores a value; we denote the value of a vertex v in the iteration k as $\mathcal{S}^k(v)$. (The fused path-based reduction of the **RADIUS** use-case that has two sources stores a pair of values.) The iterative calculation is based on the initialization function \mathcal{I} , the propagation function \mathcal{P} and the reduction function \mathcal{R} . The initialization function \mathcal{I} is a function from vertices to their initial value. For the **SSSP** use-case, \mathcal{I} is $\lambda v. \text{if } (v = s) 0 \text{ else } \perp$ that initializes the value of the source s to zero

(the some value of zero to be more precise) and the other vertices to none \perp . In each iteration, if the value of a vertex changes, its successors are notified to be active in the next iteration. As Fig. 3a shows, in an iteration $k + 1$, an active vertex v pulls the value $S^k(u)$ of each of its predecessors u . It then applies the propagation function \mathcal{P} to the value $S^k(u)$ and the edge $\langle u, v \rangle$. It then reduces using \mathcal{R} the results of propagation from the predecessors together and with the current value $S^k(v)$ of v to calculate the new value $S^{k+1}(v)$ of v . After a number of iterations, the values of the vertices converge. The calculation stops when the values of all vertices stay unchanged in two consecutive iterations.

Correctness and Synthesis. In § 5.1, for a given specification, we formalize *correctness and termination conditions* that are parametric in terms of the candidate initialization and propagation functions. We present sufficient conditions for a comprehensive set of iteration methods. As an example, we consider the pull model and illustrate one of the correctness conditions on the propagation function \mathcal{P} in Fig. 3b and Fig. 3c. Consider a vertex v and a predecessor u of v . Consider the reduction over all the paths to v that go through u . Fig. 3b shows the direct calculation where the value of the path function for each path to v is separately calculated and then the results are reduced. On the other hand, Fig. 3c shows a calculation using the propagation function \mathcal{P} where first, the values of the path function for the paths to the predecessor u are calculated and reduced, and then, the result is propagated to v . In order to correctly calculate the path-based specifications, the iterative computation requires the result of the above two calculations to be the same. Global reductions over paths should be equivalent to local propagations from predecessors. Further, to reason about termination, we formalize the termination conditions for the two iteration models in § 5.1. Iterations incrementally consider longer paths. Cycles of a graph generate an infinite number of paths and can cause divergence. However, sometimes adding longer paths has no effect on the result of the reduction. For example for the shortest path use-case SSSP (with non-negative edges), after a certain number of iterations, all the simple paths of the graph are already considered, and longer cyclic paths cannot improve the shortest path.

In § 5.2, we use the correctness conditions to synthesize correct iteration functions \mathcal{I} and \mathcal{P} . In particular, we apply type-guided enumerative synthesis to find candidates and automatic solvers to check the validity of the correctness conditions for each. The result is correct-by-construction kernel functions that can iteratively calculate path-based reductions. In § 6, we use the synthesized iteration functions to generate code for five high-performance graph computation frameworks.

3 ITERATIVE MODELS

We formalize four canonical models for iterative graph computations: the pull and push models with idempotent and non-idempotent reduction. Graph computation frameworks [Gonzalez et al. 2012; Malewicz et al. 2010; Roy et al. 2013; Shun and Blueloch 2013; Zhu et al. 2016, 2015] implement variants of these models. Later in § 5, we use them to implement path-based reductions and the correctness conditions of these implementations.

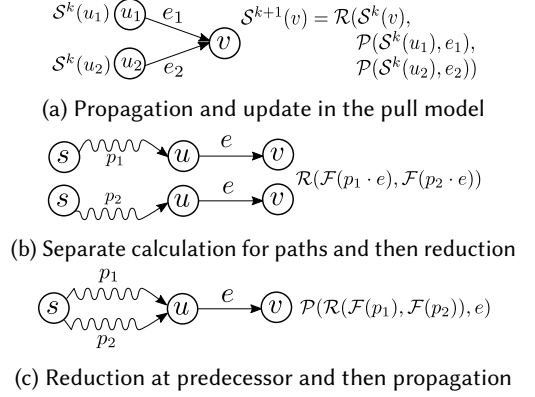


Fig. 3. The pull model and its correctness. The path $p \cdot e$ denotes the extension of path p with edge e .

$e ::= n \mid v$	Body Exp	SSSP
$e + e \mid e - e \mid -e \mid \langle e, e \rangle$		$\mathcal{I} := \lambda v. \text{ if } (v = s) 0 \text{ else } \perp$
$e * e \mid e / e \mid e = e \mid e < e$		$\mathcal{P} := \lambda n, e. n + \text{weight}(e)$
$\min(e, e) \mid \max(e, e)$		$\mathcal{R} := \lambda v, v'. \min(v, v')$
$\text{if } (e) \text{ then } e \text{ else } e$		$\mathcal{E} := \lambda n. n$
$\text{weight}(e) \mid \text{capacity}(e)$		PAGERANK
$\text{indeg}(e) \mid \text{outdeg}(e)$		$\mathcal{I} := \lambda v. 1 / V $
$\text{src}(e) \mid \text{dst}(e)$		$\mathcal{P} := \lambda n, e. n / \text{outdeg}(\text{src}(e))$
$ V $	Graph Order	$\mathcal{R} := \lambda v, v'. v + v'$
$n ::= 0 \mid 1 \mid \dots \mid \text{True} \mid \text{False}$	Literal	$\mathcal{E} := \lambda n. \gamma * n + (1 - \gamma) / V $
v	Variable	
(a) Grammar		(b) Examples

Fig. 4. (a) Grammar for kernel functions (b) Example kernel functions. (min and + filter none values \perp .)

In these models, each vertex is first initialized. Then, the value of each vertex is iteratively updated based on the values of its predecessors. In each iteration, the values of the predecessors are pulled or each predecessor pushes its value to the vertex. Then, the values of the predecessors are reduced to a single value. Before assigning the reduced value to the vertex, a final function may be applied to it. The iteration stops when the value of no vertex changes.

The iteration models are parametrized by four kernel functions: \mathcal{I} , \mathcal{P} , \mathcal{R} and \mathcal{E} . The initialization function \mathcal{I} defines the initial value for each vertex. The propagation function \mathcal{P} , given a value n and an edge e where n is the current value of the source of e , defines the value that is propagated to the destination of e . The reduction function \mathcal{R} defines how the propagated values are aggregated. The epilogue function \mathcal{E} , given an aggregated value n , defines the final update to n .

This work presents a high-level language to specify the kernel functions. It compiles kernels specified in this language to executable programs in five graph processing frameworks. The language grammar for bodies of the kernel functions is presented in Fig. 4a. Later in § 5.2, the same grammar is used by the synthesis process; given higher-level specifications, it automatically generates the kernel functions in this language. Fig. 4b shows the iterative kernel functions for two use-cases: the shortest path SSSP and the page-rank PAGERANK. For the shortest path SSSP use-case, the initialization function \mathcal{I} initializes the source vertex s to 0 and the other vertices to none \perp . The propagation function \mathcal{P} adds the value n of the predecessor with the weight of the edge e . The reduction function \mathcal{R} is the minimum (that is idempotent) and the epilogue function is the identity function. For the page-rank PAGERANK use-case, the initialization function \mathcal{I} divides the value 1 between the number of vertices $|V|$. The propagation function \mathcal{P} divides the value n of the predecessors between its successors. The reduction function \mathcal{R} is sum (non-idempotent). The epilogue function multiplies the sum with the damping factor γ and adds a constant. We now consider each model.

Pull Model. The characteristic of the pull model is that vertices pull the values of their predecessors to calculate their new values. We consider the pull model for idempotent and non-idempotent reduction functions in turn.

Pull model with idempotent reduction (pull+). The pull model for idempotent reduction is represented in Fig. 5, Def. 1. The value of the vertex v in the iteration k is represented by $S_{\text{pull}+}^k(v)$. In the beginning $k = 0$, the vertices have no value \perp . In the first iteration $k = 1$, they are initialized by the initialization function \mathcal{I} . In subsequent iterations $k + 1$, $k \geq 1$, each vertex v pulls values of its predecessors. For each predecessor u , the propagation function \mathcal{P} is applied to the value of u (from the previous iteration k) and the connecting edge $\langle u, v \rangle$. Then, as illustrated in Fig. 3a, all the

$$\text{CPreds}^k(v) = \{u \mid u \in \text{preds}(v) \wedge S^k(u) \neq S^{k-1}(u)\}$$

DEFINITION 1 (PULL (IDEMPOTENT REDUCTION)).

$$\begin{aligned} S_{\text{pull}+}^0(v) &:= \perp \\ S_{\text{pull}+}^1(v) &:= I(v) \\ S_{\text{pull}+}^{k+1}(v) &:= \begin{cases} S_{\text{pull}+}^k(v) & \text{if } \text{CPreds}^k(v) = \emptyset \\ \mathcal{E} \left[\mathcal{R} \left(S_{\text{pull}+}^k(v), \mathcal{R}_{u \in \text{preds}(v)} \mathcal{P} \left(S_{\text{pull}+}^k(u), \langle u, v \rangle \right) \right) \right] & \text{else} \end{cases} \quad k \geq 1 \end{aligned}$$

DEFINITION 2 (PULL (NON-IDEMPOTENT REDUCTION)).

$$\begin{aligned} S_{\text{pull}-}^0(v) &:= \perp \\ S_{\text{pull}-}^1(v) &:= I(v) \\ S_{\text{pull}-}^{k+1}(v) &:= \begin{cases} S_{\text{pull}-}^k(v) & \text{if } \text{CPreds}^k(v) = \emptyset \\ \mathcal{E} \left[\mathcal{R}_{u \in \text{preds}(v)} \mathcal{P} \left(S_{\text{pull}-}^k(u), \langle u, v \rangle \right) \right] & \text{else} \end{cases} \quad k \geq 1 \end{aligned}$$

DEFINITION 3 (PUSH (IDEMPOTENT REDUCTION)).

$$\begin{aligned} S_{\text{push}+}^0(v) &:= \perp \\ S_{\text{push}+}^1(v) &:= I(v) \\ S_{\text{push}+}^{k+1}(v) &:= \mathcal{E}(S_n), \quad k \geq 1 \quad \text{where} \\ &\quad \text{let } \{u_0, \dots, u_{n-1}\} := \text{CPreds}^k(v) \text{ in} \\ &\quad S_0 := S_{\text{push}+}^k(v) \\ &\quad S_{i+1} := \mathcal{R} \left(S_i, \mathcal{P} \left(S_{\text{push}+}^k(u_i), \langle u_i, v \rangle \right) \right) \end{aligned}$$

DEFINITION 4 (PUSH (NON-IDEMPOTENT REDUCTION)).

$$\begin{aligned} S_{\text{push}-}^0(v) &:= \perp \\ S_{\text{push}-}^1(v) &:= I(v) \\ S_{\text{push}-}^{k+1}(v) &:= \mathcal{E}(S_n), \quad k \geq 1 \quad \text{where} \\ &\quad \text{let } \{u_0, \dots, u_{n-1}\} := \text{preds}(v) \text{ in} \\ &\quad S_0 := \perp \\ &\quad S_{i+1} := \mathcal{R} \left(S_i, \mathcal{P} \left(S_{\text{push}-}^k(u_i), \langle u_i, v \rangle \right) \right) \end{aligned}$$

Fig. 5. Four Iterative Reduction Methods. (GRAFS also incorporates another variant of Push, Non-idempotent Reduction (appendix § 3.1.2)). $\text{CPreds}^k(v)$: The predecessors of the vertex v that changed in the iteration k

propagated values are reduced by \mathcal{R} with each other and then with the previous value of v . Finally, the application of the epilogue function to the reduced value results in the new value of v . As an optimization, the above update is performed only if the value of at least one predecessor has been updated in the previous iteration.

Pull model with non-idempotent reduction (pull-). The pull model for non-idempotent reduction is represented in Fig. 5, Def. 2. The value of the vertex v in the iteration k is represented as $S_{\text{pull}-}^k(v)$. Similar to the pull model for idempotent reduction, the values from predecessors are propagated and reduced. The value that each vertex stores is a reduction of a set of values. Consider a vertex v a predecessor u of v . Assume that the value of u represents the reduction of a set S of elements. After the value of u is propagated to v , the value of v includes the reduction of S . Assume that the value of u is updated to represent the reduction more elements. Since the reduction is non-idempotent, propagating the new value of u to v and reducing it with the current value of v results in the two times reduction of S in v . Therefore, to avoid this duplicated reduction, the difference of this model with the previous model is that after reducing the propagated values, the result is not reduced with the previous value of the vertex.

Push Model. In the pull model above, each vertex itself pulled values from its predecessors. In contrast, in the push model, the predecessors push values to the vertex when they are updated. We consider the push model for idempotent and non-idempotent reduction functions in turn.

Push model with idempotent reduction (push+). The push model for idempotent reduction is represented in Fig. 5, Def. 3. The value of the vertex v in the iteration k is represented with

$S_{\text{push}+}^k(v)$. In the beginning $k = 0$, the vertices have no value \perp . In the first iteration $k = 1$, they are initialized by the initialization function \mathcal{I} . In subsequent iterations $k + 1$, $k \geq 1$, for each vertex v , the predecessors $\{u_0, \dots, u_{n-1}\}$ that have been changed in the previous iteration independently propagate their values and reduce it with the current value of v . Since the reduction function is commutative and associative, the predecessors can apply their updates in any order. In each iteration, the initial value S_0 of v is its value in the previous iteration k . For each changed predecessor u_i , the propagation function \mathcal{P} is applied to the value of u_i (from the previous iteration k) and the connecting edge $\langle u_i, v \rangle$. The result is then reduced with the current value S_i of v to calculate its new value S_{i+1} . Propagation and reduction by the last changed predecessor u_{n-1} results in the value S_n . The final value of v in the iteration is the application of the epilogue \mathcal{E} to S_n .

Push model with non-idempotent reduction (push-). This model works for non-idempotent (in addition to idempotent) reduction functions. The iteration model is represented in Fig. 5, Def. 4. Let the value of the vertex v in the iteration k be represented as $S_{\text{push-}}^k(v)$. Since the reduction function may not be idempotent, in contrast to the previous model, vertices start from the none value \perp and all the predecessors u_i propagate their values in each iteration. For each predecessor u_i , the propagate function \mathcal{P} is applied to the latest value $S_{\text{push-}}^k(u_i)$ of u_i and the edge $\langle u_i, v \rangle$. The resulting value is reduced with the current value of v . We note that this variant makes all vertices active during an iteration; GRAFS also incorporates another variant (appendix § 3.1.2) where only the vertices whose values change are active and propagate their values. In this variant, every active predecessor u_i first rollbacks its previous update before applying its new update.

The iteration models that we saw here are *synchronous*. In the synchronous model, vertices store the previous in addition to the new value to propagate the previous value. In the *asynchronous* model, however, each vertex stores one value, and vertices can propagate intermediate values. We present four asynchronous models and their correctness in the appendix § 3.1.3. Further, we present streaming iteration models and their correctness in the appendix § 3.1.4.

4 SPECIFICATION AND FUSION

We define the core specification language and the semantics-preserving fusion transformations:

4.1 Core Specification Language

To present the crux of the fusion transformations, we define a core specification language in Fig. 6. It features both reduction over paths and reduction over vertices. A computation can be specified as a reduction r over the values of *vertices*. The value of vertices can be specified as a nested reduction m over the *paths* to each vertex. More elaborate computations can be specified by nested path-based computations and applying operations between multiple vertex-based computations. We will visit each term type in turn.

Vertex-based and path-based reductions. A vertex-based reduction $\mathcal{R} m$ applies a reduction function \mathcal{R} to the result of path-based reductions m over all vertices V . The function \mathcal{R} is a commutative and associative function such as \min , and \sum . Larger vertex-based reductions $r \oplus r'$ can be constructed using the operators \oplus . A path-based reduction $\mathcal{R} \mathcal{F}(p)$ applies a reduction function \mathcal{R} to the result of the function \mathcal{F} on the paths P . Similar to vertex-based reductions, larger path-based reductions $m \oplus m'$ can be constructed using the operators \oplus . The path function \mathcal{F} is the length, weight, or capacity of the path. The set of paths P can be either Paths that denotes all the paths to each vertex, or the restricted paths $\text{args } \mathcal{R} \mathcal{F}(p)$ where $\mathcal{R} \in \{\min, \max\}$ that denotes the paths in P whose \mathcal{F} value is the minimum or maximum. Restricted paths lead to nested path-based computations.

Let forms. The fusion transformations use let terms to factor reductions. Factored reductions are conducive to fusion. As shown in Fig. 6, the terms m and r both have let forms. The m term constructor $\text{ilet } X := M \text{ in } e$ binds variables X to path-based reductions M for the expression e . The expression e can apply operators \oplus to the variables X . Both the variables X and reductions M can be inductively constructed as pairs. A single path-based reduction M is simply represented as $\mathcal{R}\mathcal{F}$ where \mathcal{R} is the reduction function and \mathcal{F} is the path function. Similarly, the triple-let r constructor $\text{ilet } X := M \text{ in mlet } X' := E \text{ in rlet } X'' := R \text{ in } e$ binds variables X to path-based reductions M , variables X' to expressions E (on X), and variables X'' to vertex-based reductions R (on X'). A triple-let term represents an r term as path-based reductions, then mappings on the results, and finally vertex-based reductions on the results. We will see that this form enables fusion (§ 4.2) and can be directly implemented (§ 6). Similar to M , the vertex-based reductions R can be inductively constructed as pairs. A single vertex-based reduction R is $\mathcal{R} \langle \bar{x} \rangle$ that is a reduction over tuples of vertex variables $\langle \bar{x} \rangle$ (or $\mathcal{R} \langle \bar{d} \rangle$ after the variables are substituted with map values d from vertices to values). To concisely represent the fusion rules, we define the context \mathbb{R} to abstract the surrounding term where a term r appears. Similarly, we define the contexts \mathbb{M} , $\mathbb{M}s$, and $\mathbb{R}s$ for the terms m , M and R .

Semantics and Compositionality. In the appendix § 2.1, we defined a denotational semantics for the language presented in Fig. 6. It defines the semantics $\llbracket \cdot \rrbracket$ of each term type. The domain \mathcal{D}_m of a path-based computation m on a graph g is a finite map from each vertex of g to natural numbers $V(g) \mapsto \mathbb{N}$ and \perp (for undefined computation). The domain \mathcal{D}_r of a vertex-based computation r is the natural numbers \mathbb{N} and \perp (for undefined computation). We prove that the semantics is compositional. If two terms are semantically equivalent, replacing one with the other in any context is semantics-preserving. Compositionality of the semantics is used to prove that the fusion transformations are semantic-preserving. The following theorem states compositionality for r . (The proofs and other lemmas are available in the appendix § 4.2.)

LEMMA 1 (COMPOSITIONALITY). *For all r, r' and \mathbb{R} , if $\llbracket r \rrbracket = \llbracket r' \rrbracket$ then $\llbracket \mathbb{R}[r] \rrbracket = \llbracket \mathbb{R}[r'] \rrbracket$.*

4.2 Fusion

We now present the fusion transformations. Fusion reduces computation time by combining separate reductions into a single reduction. The transformations have three main forms: fusion of nested path-based reductions, fusion of pairs of path-based reductions, and fusion of pairs of vertex-based reductions. The result of fusion is an equivalent specification in the triple-let form with separate terms for path-based reduction, mapping over vertices and vertex-based reduction.

The fusion rules are presented in Fig. 8. The top-level fusion relation \Rightarrow_r is called r -fusion and transforms an r term to another. The other fusion relations \Rightarrow_m , \Rightarrow_M , and \Rightarrow_R are called m -fusion, M -fusion and R -fusion, and transform m , M and R terms respectively. The rule **FMINR** states that m -fusions can be applied to m terms that appear in the context of r terms. (Both $\mathbb{M}[m_1]$ and $\mathbb{M}[m_2]$ in this rule are r terms.) We consider m -fusions first. The rule **FMINM** states that m -fusions can be applied to m terms in the context of other m terms.

Fusing nested path-based reductions. The rule **FPNEST** m -fuses nested path-based reductions to flat reductions. Consider the nested path-based reduction $\mathcal{R} \mathcal{F}(p)$ where the set of paths P' is another path-based reduction $\arg s \mathcal{R}' \mathcal{F}'(p)$ where \mathcal{R}' is min or max. Let us assume that \mathcal{R}' is min.

A straightforward calculation computes \mathcal{F}' on the paths P and finds the subset of paths P' with the minimum value, and then computes \mathcal{F} on the paths P' and reduces them by \mathcal{R} . An optimized calculation can compute both \mathcal{F}' and \mathcal{F} on the paths P simultaneously and only consider the pairs with the minimum first element to calculate the reduction \mathcal{R} over the second elements. To calculate

the values of the path functions \mathcal{F} and \mathcal{F}' , this approach enumerates paths only once instead of twice. (We will see in § 5.1 that the calculation can further avoid the explicit enumeration of paths.) Therefore, the two reductions can be fused into one reduction as $\text{ilet } \langle x, x' \rangle := \mathcal{R}'' \mathcal{F}''(p')$ in x' .

The new path function $\mathcal{F}''(p')$ returns the pair of values $\mathcal{F}'(p')$ and $\mathcal{F}(p')$. The new reduction function \mathcal{R}'' considers the first element of the two input pairs and if the first element of one input is (strictly) smaller than the other, that input is returned. That input takes over because the set of paths for the reduction \mathcal{R} are only those with the minimum value for \mathcal{F}' . On the other hand, if the first elements of the inputs are equal, their second elements are reduced by \mathcal{R} to make the second element of the output pair. The rule **FPNEST** can be repeatedly applied to a deeply nested path-based reduction to flatten it to a reduction over the basic paths term *Paths*.

Factoring, pairing and fusing path-based reductions. The rule **FPRED** factors out a flat reduction to an equivalent let form. The rule **FILETBIN** fuses an operation between two let terms to a single let term. It pairs the factored reductions M_1 and M_2 of the two let terms to keep the reductions of the resulting term factored. The condition of the rule prevents the free variables of the expression of one term from clashing with the bound variables of another. The rule **FMINILET** allows the factored reductions M in the context of a let term to be fused. The rule **FMPAIR** M -fuses a pair of factored reductions $\langle \mathcal{R} \mathcal{F}, \mathcal{R}' \mathcal{F}' \rangle$ to a single reduction $\mathcal{R}'' \mathcal{F}''$ that calculates the two reductions simultaneously. The path function \mathcal{F}'' returns the pair of the results of \mathcal{F} and \mathcal{F}' . Similarly, the reduction function \mathcal{R}'' returns a pair: the reduction of the first elements by \mathcal{R} and the second elements by \mathcal{R}' .

Factoring into, pairing and fusing triple-let terms. The rules above can factor all path-based reductions m to the let form and fuse factored reductions to a single one. The next rule **FVRED** expects path-based reductions

r	$:= \mathcal{R} m \mid r \oplus r \mid x \mid$ \vee $\text{ilet } X := M \text{ in}$ $\text{mlet } X := E \text{ in}$ $\text{rlet } X := R \text{ in } e$	Vertex-based Red.
m	$:= \mathcal{R} \mathcal{F}(p) \mid m \oplus m \mid$ $p \in P$ $\text{ilet } X := M \text{ in } e \mid x$	Path-based Red.
P	$:= \text{Paths} \mid \text{args} \mathcal{R} \mathcal{F}(p)$ $p \in P$	Paths
\mathcal{R}	$:= \min \mid \max \mid \vee \mid \wedge \mid \Sigma$	Reduction Fun.
\mathcal{F}	$:= \text{length} \mid \text{weight} \mid \text{capacity}$	Path Fun.
\oplus	$:= \min \mid \max \mid \wedge \mid \vee \mid + \mid$ $- \mid \times \mid / \mid = \mid < \mid >$	Operation
p		Path Variable
x		Variable
e	$:= e \oplus e \mid x$	
X	$:= \langle X, X \rangle \mid x$	
M	$:= \langle M, M \rangle \mid \mathcal{R} \mathcal{F}$	
R	$:= \langle R, R \rangle \mid \mathcal{R} \langle \bar{x} \rangle \mid \mathcal{R} \langle \bar{d} \rangle$	
E	$:= \langle E, E \rangle \mid e$	
\mathbb{R}	$:= [] \mid \mathbb{R} \oplus r \mid r \oplus \mathbb{R}$	Context for r
\mathbb{M}	$:= [] \mid \mathcal{R} \mathbb{M} \mid \mathbb{M} \oplus m \mid m \oplus \mathbb{M}$ \vee	Context for m
$\mathbb{M}s$	$:= [] \mid \langle \mathbb{M}s, M \rangle \mid \langle M, \mathbb{M}s \rangle \mid$ $\text{ilet } X := \mathbb{M}s \text{ in } e \mid$ $\text{ilet } X := \mathbb{M}s \text{ in mlet } X := E \text{ in rlet } X := R \text{ in } e$	Context for M
$\mathbb{R}s$	$:= [] \mid \langle \mathbb{R}s, R \rangle \mid \langle R, \mathbb{R}s \rangle \mid$ $\text{ilet } X := M \text{ in mlet } X := E \text{ in rlet } X := \mathbb{R}s \text{ in } e$	Context for R
n		Value
v		Vertex Value
$d: \mathcal{D}_m$	$:= (V(g) \mapsto \mathbb{N}) \cup \{\perp\}$	Sem. Dom. of m
$n_\perp: \mathcal{D}_r$	$:= \mathbb{N} \cup \{\perp\}$	Sem. Dom. of r

Fig. 6. Core specification language

to be in the let form. It transforms vertex-based reductions that are applied to path-based reductions to an equivalent triple-let form. The triple-let form factors both path-based and vertex-based reductions in separate let parts: the first and third lets respectively. The rule **FLETSBIN** fuses an operation between two triple-let terms to a single triple-let term. It pairs the factored path-based reductions M , expression E , and vertex-based reduction R of the two terms. The rule **FMINLETS** allows the factored path-based reductions M in the context of a triple-let term to be M -fused. (As we saw

above, the rule **FMPAIR** presents M -fusions.) The rule **FRinLETS** allows the factored vertex-based reductions R in the context of a triple-let term to be R -fused.

Fusing vertex-based reductions. The rule **FRPAIR** presents R -fusions. It fuses a pair of R reductions $\langle \mathcal{R}_1 x_1, \mathcal{R}_2 x_2 \rangle$ to a single R reduction $\mathcal{R}_3 \langle x_1, x_2 \rangle$. Given two pairs, the reduction function \mathcal{R}_3 returns a pair: the reduction of the first elements by \mathcal{R}_1 and the second elements by \mathcal{R}_2 .

The fusion presented above is semantic-preserving. Terms are only fused into other terms with the same semantics. The following theorem states the semantics-preservation property of fusion. (The proofs are available in the appendix § 4.3.)

THEOREM 1 (SEMANTICS-PRESERVING FUSION). *For all r_1 and r_2 , if $r_1 \Rightarrow_r r_2$ then $\llbracket r_1 \rrbracket = \llbracket r_2 \rrbracket$.*

4.3 Extensions

We now consider extensions to the core syntax and the fusion rules.

Common Operation Elimination. Fusion factors the path-based reduction, vertex-based mappings and vertex-based reductions in the triple-let form. This form facilitates common operation elimination. For example, if a path-based reduction is calculated twice and assigned to two sets of variables, the extra calculation can be eliminated and the result of one calculation can be assigned to both sets of variables. The elimination rules are available in the appendix § 2.2.1.

Domain. The scalar semantic domain of the core language was confined to the natural numbers. The domain can be simply extended to booleans, vertex identifiers and also sets of values. The reduction operations are extended with union \cup and intersection \cap and the path functions are extended with head and penultimate. The function head returns the identifier of the head vertex of the path and the function penultimate returns the identifier of the penultimate (that is the vertex before the last) of the path. *Unary operations and Literals.* The path-based reductions m and vertex-based reductions r can be simply extended with unary operations and literals. Their supporting fusion rules are available in the appendix § 2.2.3.

Vertex Variables. We extend the core syntax with path terms $\text{Paths}(v, v')$ and $\text{Paths}(v)$ that can specify vertex variables as source and destination. The term $\text{Paths}(v, v')$ specifies the set of paths from the source v to the destination v' , and the term $\text{Paths}(v)$ specifies the set of paths from any source to the destination v . Thus, the source s of a path-based reduction can be either a vertex v or none \perp . A factored path-based reduction $\mathcal{R} \mathcal{F}$ carries its configuration c . The configuration c is a source, or a pair of other configurations. We also extend the syntax with vertex-based reductions $\mathcal{R} m$ that can bind the vertex variable v . (We define this syntax extension and its fusion rules in the appendix § 2.2.4.)

Syntactic Sugar. Syntactic sugar enable concise specifications. For example, the term $\mathcal{F}(\arg \mathcal{R} \mathcal{F}'(p))$ where \mathcal{R} is either min or max first finds a path p in P with the minimum or maximum value for the function \mathcal{F}' and then returns the result of applying \mathcal{F} to p . It is used to specify the **BFS** use-case. The rule **FMRED** expands this term to a path-based reduction in the let form $\text{ilet } \langle x, x' \rangle := \mathcal{R}' \mathcal{F}''(p) \text{ in } x'$. The path function \mathcal{F}'' returns the pair of the results of \mathcal{F}' and \mathcal{F} . The reduction function \mathcal{R}' returns the input pair with the minimum or maximum first element.

$$\begin{aligned}
 \text{FMRED} \\
 \mathcal{F}(\arg \mathcal{R} \mathcal{F}'(p)) &:= \text{ilet } \langle x, x' \rangle := \mathcal{R}' \mathcal{F}''(p) \text{ in } x' \quad \text{where } \mathcal{R} \in \{\min, \max\} \\
 \mathcal{F}'' &:= \lambda p. \langle \mathcal{F}'(p), \mathcal{F}(p) \rangle \quad \mathcal{R}'(\langle a, b \rangle, \langle a', b' \rangle) := \text{if } (\mathcal{R}(a, a') = a) \text{ then } \langle a, b \rangle \text{ else } \langle a', b' \rangle
 \end{aligned} \tag{7}$$

We discuss the syntactic sugar for (1) cardinality $|P|$, (2) vertex-based reduction over a given subset of vertices $\mathcal{R}_{v \in \{v_1, \dots, v_n\}} m$ and (3) vertex-based reduction constrained by a path-based reduction

$\mathcal{R}_{v \in V \wedge m'} m$ (that are used to specify the use-cases **NSP**, **RADIUS**, and **DS**) in Fig. 1.

Nested Triple-lets. The core syntax supports expressions that can be fused to a single iteration-map-reduce triple-let term. We extend the core syntax to support nested vertex-based reductions, and extend the fusion rules to fuse nested reductions. For example, the use-case RDS that we saw in Fig. 1 uses the vertex-based reduction **RADIUS** as a nested term. Nested triple-let terms can be translated to a sequence of iteration-map-reduce rounds on the graph. (In the appendix § 2.2.6, we define the extension and show that RDS is fused to two rounds of iteration-map-reduce.)

We saw an example fusion in Fig. 2. More examples are available in the appendix § 2.3.

5 MAPPING SPECIFICATION TO ITERATION-MAP-REDUCE

In the previous section, we saw a fusion process that transforms specifications to the following triple-let form. As we saw in the final term in Fig. 2, the fusion results in the triple-let form shown in Fig. 7. It has three separate operations: the path-based reduction, mapping expressions over their results, and the subsequent vertex-based reduction. The three let parts can be directly mapped to three computation primitives: iteration, map and reduce. Each vertex stores the variables X and X' . The first let is mapped to an iterative calculation for the path-based reduction that results in values for the variables X in each vertex. The second let is mapped to a map operation over vertices: given the values of the variables X in each vertex, the map operation calculates the values of the expressions E and stores the results in the variables X' for the vertex. The third let is mapped to a reduction operation over vertices: given the values of the variables $\overline{x'}$ in X' in each vertex, the reduction operation reduces the values of $\langle \overline{x'} \rangle$ for all vertices and stores the results in the global variables X'' . Finally, the expression e is calculated based on the values of X'' .

The two latter primitives, vertex-based mapping and reduction, can be implemented by a traversal over vertices. Since the mapping and the reduction both traverse the vertices, a simple optimization is to perform them in the same pass. We consider how path-based reductions can be implemented. We saw the iterative computation models in § 3. Now, we present how they can be instantiated to implement path-based reductions. We first present the correctness conditions of the iterative models to calculate path-based reductions (§ 5.1), and then present the synthesis of iteration kernel functions based on the correctness conditions (§ 5.2).

$$\begin{aligned} &\text{ilet } X := \mathcal{R} \mathcal{F} \text{ in} \\ &\text{mlet } X' := E \text{ in} \\ &\text{rlet } X'' := \mathcal{R}' \langle \overline{x'} \rangle \text{ in } e \end{aligned}$$

Fig. 7. Triple-let form

5.1 Iterative Path-based Reduction and its Correctness

We now present the iterative calculation of path-based reductions. We consider both the pull and push models with both idempotent and non-idempotent reduction. For each model, we present correctness and termination conditions.

Specification. In Fig. 7, factored path-based reductions in the triple-let terms have the form $\mathcal{R} \mathcal{F}$. Considering a single reduction, c is either none \perp or a source vertex s . (We discuss a similar treatment for general configurations in the appendix § 3.1.5.) The factored reduction for the former (with no source) is simply unrolled to $\mathcal{R}_{p \in \text{Paths}(v)} \mathcal{F}(p)$ and the latter (with the source s) is unrolled to $\mathcal{R}_{p \in \{p \mid p \in \text{Paths}(v) \wedge \text{head}(p)=s\}} \mathcal{F}(p)$. We capture both of these reductions as the following general specification where the condition $C(p)$ is True for the former and $\text{head}(p) = s$ for the latter.

DEFINITION 5 (SPECIFICATION). $\text{Spec}(v) = \mathcal{R}_{p \in \{p \mid p \in \text{Paths}(v) \wedge C(p)\}} \mathcal{F}(p)$

$$\begin{array}{c}
\text{FMINR} \\
\frac{m_1 \Rightarrow_m m_2}{\mathbb{M}[m_1] \Rightarrow_r \mathbb{M}[m_2]} \\
\\
\text{FMINM} \\
\frac{m_1 \Rightarrow_m m_2}{\mathbb{M}[m_1] \Rightarrow_m \mathbb{M}[m_2]} \\
\\
\text{FPRED} \\
\frac{\mathcal{R} \quad \mathcal{F}(p)}{p \in \text{Paths} \Rightarrow_m} \\
\text{ilet } x := \mathcal{R} \mathcal{F} \text{ in } x \\
\\
\text{FMINLET} \\
\frac{M_1 \Rightarrow_M M_2}{\text{ilet } X := \mathbb{M}s[M_1] \text{ in } e \Rightarrow_m \text{ilet } X := \mathbb{M}s[M_2] \text{ in } e} \\
\\
\text{FLETsBIN} \\
\left(\text{ilet } X_1 := M_1 \text{ in } e_1 \oplus \left(\text{mlet } X'_1 := E_1 \text{ in } \text{rlet } X''_1 := R_1 \text{ in } e_1 \right) \right) \Rightarrow_r \left(\text{ilet } X_2 := M_2 \text{ in } e_2 \oplus \left(\text{mlet } X'_2 := E_2 \text{ in } \text{rlet } X''_2 := R_2 \text{ in } e_2 \right) \right) \\
\text{if } \begin{array}{l} \text{free}(E_1) \cap X_2 = \\ \text{free}(E_2) \cap X_1 = \\ \text{free}(R_1) \cap X'_2 = \\ \text{free}(R_2) \cap X'_1 = \\ \text{free}(e_1) \cap X''_2 = \\ \text{free}(e_2) \cap X''_1 = \emptyset \end{array} \\
\\
\text{FMINLETS} \\
\frac{M_1 \Rightarrow_M M_2}{\left(\text{ilet } X := \mathbb{M}s[M_1] \text{ in } \text{mlet } X' := E \text{ in } \text{rlet } X'' := R \text{ in } e \right) \Rightarrow_r \left(\text{ilet } X := \mathbb{M}s[M_2] \text{ in } \text{mlet } X' := E \text{ in } \text{rlet } X'' := R \text{ in } e \right)} \\
\\
\text{FRINLETS} \\
\frac{R_1 \Rightarrow_R R_2}{\left(\text{ilet } X := M \text{ in } \text{mlet } X' := E \text{ in } \text{rlet } X'' := \mathbb{R}s[R_1] \text{ in } e \right) \Rightarrow_r \left(\text{ilet } X := M \text{ in } \text{mlet } X' := E \text{ in } \text{rlet } X'' := \mathbb{R}s[R_2] \text{ in } e \right)} \\
\\
\text{FRPAIR} \\
\frac{\langle \mathcal{R}_1 x_1, \mathcal{R}_2 x_2 \rangle \Rightarrow_R \mathcal{R}_3 \langle x_1, x_2 \rangle}{\text{where } \mathcal{R}_3(\langle a, b \rangle, \langle a', b' \rangle) := \langle \mathcal{R}_1(a, a'), \mathcal{R}_2(b, b') \rangle}
\end{array}$$

FPNEST
 $\frac{\mathcal{R} \quad \mathcal{F}(p') \Rightarrow_m \text{ilet } \langle x, x' \rangle := \mathcal{R}'' \mathcal{F}''(p) \text{ in } x'}{p' \in \text{args } \mathcal{R}' \mathcal{F}'(p) \Rightarrow_m}$
 $\text{where } \mathcal{R}' \in \{\min, \max\}$
 $f'' := \lambda p. \langle \mathcal{F}'(p), \mathcal{F}(p) \rangle$
 $\mathcal{R}''(\langle a, b \rangle, \langle a', b' \rangle) :=$
 $\text{if } (a = a') \text{ then } \langle a, \mathcal{R}(b, b') \rangle$
 $\text{else if } (\mathcal{R}'(a, a') = a) \text{ then } \langle a, b \rangle \text{ else } \langle a', b' \rangle$

FILETBIN
 $\frac{(\text{ilet } X_1 := M_1 \text{ in } e_1) \oplus (\text{ilet } X_2 := M_2 \text{ in } e_2)}{\Rightarrow_m}$
 $\text{ilet } \langle X_1, X_2 \rangle := \langle M_1, M_2 \rangle \text{ in } e_1 \oplus e_2$
 $\text{if } \begin{array}{l} \text{free}(e_1) \cap X_2 = \emptyset \\ \text{free}(e_2) \cap X_1 = \emptyset \end{array}$

FVRED
 $\frac{\mathcal{R} \quad (\text{ilet } X := \mathcal{R}' \mathcal{F} \text{ in } e)}{\vee \Rightarrow_r}$
 $\text{ilet } X := \mathcal{R}' \mathcal{F} \text{ in}$
 $\text{mlet } x := e \text{ in}$
 $\text{rlet } x' := \mathcal{R} x \text{ in } x'$

Fig. 8. Fusion Rules

The reduction function \mathcal{R} returns \perp on an empty set and returns the single element on a singleton set. We will see that the reduction function \mathcal{R} is associative and commutative. Thus, the reduction on a set of values is the result of applying \mathcal{R} to the set in any order.

Model Instantiation. Explicitly calculating the set of paths is prohibitively inefficient. Instead, path-based reductions are calculated iteratively based on the iterative models that we saw in § 3. The iterative models are parametric in terms of the kernel functions \mathcal{I} , \mathcal{P} (and \mathcal{B}), \mathcal{R} , \mathcal{E} . We will see in § 5.2 that the kernel functions \mathcal{I} , \mathcal{P} , \mathcal{B} and \mathcal{R} can be automatically synthesized from the functions \mathcal{F} and \mathcal{R} of the given path-based reduction. The epilogue function \mathcal{E} is simply instantiated to the identity function. In this subsection, we consider the correctness conditions on the kernel functions

\mathcal{I} , \mathcal{P} , \mathcal{B} and \mathcal{R} such that the iterative models calculate the specified path-based reduction. The automatic synthesis is guided by these conditions.

Correctness. The iterative models calculate the value $\mathcal{S}^k(v)$ of each vertex v in iterations k by propagating the values of its neighbor vertices. The iteration stops when the value of no vertex changes. The values of the vertices $\mathcal{S}^k(v)$ are expected to converge to the specification $\text{Spec}(v)$. We show the correctness in two steps. First, we show that under certain conditions, at the end of each iteration k , the value $\mathcal{S}^k(v)$ of each vertex v is equal to the iteration specification $\text{Spec}^k(v)$ for the iteration k . The iteration specification $\text{Spec}^k(v)$ is defined as the result of reduction over paths of length less than k .

DEFINITION 6. $\text{Spec}^k(v) = \mathcal{R}_p \in \{p \mid p \in \text{Paths}(v) \wedge C(p) \wedge \text{length}(p) < k\} \mathcal{F}(p)$

Second, we show that under certain conditions, there is an index k where $\text{Spec}^k(v)$ and $\text{Spec}^{k+1}(v)$ are equal with each other and $\text{Spec}(v)$ as well. These two steps together show that the values of vertices $\mathcal{S}^k(v)$ eventually converge to $\text{Spec}(v)$. We now consider the four variants of the iterative models. The informal and formal proofs are available in the appendix § 3.1 and 4.4 respectively.

Pull Model. We consider the correctness of the pull model to calculate path-based reductions. We look at idempotent and non-idempotent reduction functions in turn.

The correctness of the pull models is dependent on the conditions $\mathbb{C}_1 - \mathbb{C}_5$ and $\mathbb{C}_7 - \mathbb{C}_{10}$ that are presented in Fig. 9; we explain each condition in turn. The conditions \mathbb{C}_1 and \mathbb{C}_2 require the correctness of initialization in the first iteration. According to $\text{Spec}^k(v)$ (Def. 6), in the first iteration $k = 1$, for each vertex v , the value of only the paths to v should be considered that (1) have length $l < 1$, that is the single path $\langle v, v \rangle$ of zero length and (2) that satisfy the path condition C . Therefore, if the path condition C holds on the path $\langle v, v \rangle$, the value of the initialization function \mathcal{I} should be $\mathcal{F}(\langle v, v \rangle)$; otherwise, it should be none \perp . The conditions \mathbb{C}_3 and \mathbb{C}_5 state the requirements for the propagation function \mathcal{P} . The condition \mathbb{C}_3 : It simply states that if the value of the vertex is none \perp , the propagated value should be none \perp as well. The condition \mathbb{C}_4 : We saw an illustration for \mathbb{C}_4 in Fig. 3b and Fig. 3c. For a path p , we call the value of \mathcal{F} on p , the path value of p . The condition \mathbb{C}_4 states that if two paths p_1 and p_2 end in a vertex u and there is an edge $\langle u, v \rangle$ from u to a vertex v , then reducing the path values of p_1 and p_2 and then propagating the result through $\langle u, v \rangle$ is the same as reducing the path values of the two extended paths $p_1 \cdot \langle u, v \rangle$ and $p_2 \cdot \langle u, v \rangle$. (The path $p \cdot e$ denotes the extension of the path p at the end with the edge e .) Intuitively, this condition states that the local reduction and propagation of the iterative models effectively calculate reduction over paths. The condition \mathbb{C}_5 : Vertices that have only a single incoming path p do not receive multiple values to be reduced. For such vertices, \mathbb{C}_5 states that the propagation of the path value of p over the outgoing edge e is equal to the path value of the extended path $p \cdot e$. The condition $\mathbb{C}_7 - \mathbb{C}_{10}$ state the required properties of the reduction function \mathcal{R} . The none value \perp should be the identity value of \mathcal{R} , and \mathcal{R} should be commutative, associative and idempotent. For example, given the factored path-based reduction \min_s length for the shortest path use-case **SSSP**, the correct kernel functions that we saw in Fig. 4 satisfy the conditions above.

Pull model with idempotent reduction. The following theorem states that if the conditions above hold, then the value $\mathcal{S}_{\text{pull}+}^k(v)$ that the pull model with idempotent reduction (Def. 1) calculates complies with the specification $\text{Spec}^k(v)$.

THEOREM 2 (CORRECTNESS OF PULL (IDEMPOTENT REDUCTION)). *For all $\mathcal{R}, \mathcal{F}, C, \mathcal{I}, \mathcal{P}$, and $k \geq 1$, if the conditions $\mathbb{C}_1 - \mathbb{C}_9$ hold, then $\mathcal{S}_{\text{pull}+}^k(v) = \text{Spec}^k(v)$.*

Pull model with non-idempotent reduction. We saw the pull model with non-idempotent reduction $\mathcal{S}_{\text{pull}+}^k(v)$ in Def. 2. We show that it can correctly calculate path-based reductions with

non-idempotent (in addition to idempotent) reduction functions. For instance, consider the factored path-based reduction $\sum_s 1$ that counts the number of paths from the source s ; the reduction function \sum is non-idempotent. The initialization function is instantiated to $\mathcal{I} = \lambda v. 1$ and the propagation function is instantiated to $\mathcal{P} = \lambda n, e. n$ that simply propagates the value of the predecessor.

The following theorem states that if the conditions above except idempotency hold and the given source vertex is not on any cycle then the pull model with non-idempotent reduction $\mathcal{S}_{\text{pull-}}^k(v)$ complies with the specification $\text{Spec}^k(v)$.

THEOREM 3 (CORRECTNESS OF PULL (NON-IDEMPOTENT REDUCTION)). *For all $\mathcal{R}, \mathcal{F}, \mathcal{I}, \mathcal{P}, k \geq 1$, and s , let $C(p) = (\text{head}(p) = s)$, if the conditions $\mathbb{C}_1 - \mathbb{C}_8$ hold, and s is not on any cycle, $\mathcal{S}_{\text{pull-}}^k(v) = \text{Spec}^k(v)$.*

Push Model. We now consider the correctness of the push model to calculate path-based reductions.

Push model with idempotent reduction. The following theorem states that if the conditions $\mathbb{C}_1 - \mathbb{C}_9$ hold, the value $\mathcal{S}_{\text{push+}}^k(v)$ that the push model with idempotent reduction (Def. 3) calculates complies with the specification $\text{Spec}^k(v)$.

THEOREM 4 (CORRECTNESS OF PUSH (IDEMPOTENT REDUCTION)). *For all $\mathcal{R}, \mathcal{F}, \mathcal{C}, \mathcal{I}, \mathcal{P}$, and $k \geq 1$, if the conditions $\mathbb{C}_1 - \mathbb{C}_9$ hold, $\mathcal{S}_{\text{push+}}^k(v) = \text{Spec}^k(v)$.*

Push model with non-idempotent reduction.

Similarly, the following theorem states the correctness of the model with non-idempotent reduction (Def. 4).

THEOREM 5 (CORRECTNESS OF PUSH (NON-IDEMPOTENT REDUCTION)). *For all $\mathcal{R}, \mathcal{F}, \mathcal{I}, \mathcal{P}, k \geq 1$, and s , let $C(p) = (\text{head}(p) = s)$, if the conditions $\mathbb{C}_1 - \mathbb{C}_8$ hold, and s is not on any cycle, $\mathcal{S}_{\text{push-}}^k(v) = \text{Spec}^k(v)$.*

Termination. We showed that all the four iteration models comply with the iteration specification $\text{Spec}^k(v)$ in every iteration k . We now show that under certain conditions, there exists an iteration k where $\text{Spec}^k(v)$ (Def. 6) stays unchanged and converges to the original specification $\text{Spec}(v)$ (Def. 5). The observation is that iterations incrementally consider longer paths; however, longer paths do not necessarily yield new information. For example, in the shortest path use-case **SSSP**, after considering all the simple paths, the longer paths (that are cyclic) cannot lead to shorter paths (in graphs with non-negative edges). Given a path p , we call the path that results from removing its cycles the simplification $\text{simple}(p)$ of p . In the shortest path use-case **SSSP**, the reduction function \mathcal{R} is \min and the path function \mathcal{F} is weight . Reducing the \mathcal{F} value of $\text{simple}(p)$ with the \mathcal{F} value of p results in the former. In other words, simplified paths are enough to arrive at the same

Initialization:

$$\mathbb{C}_1: \forall v. C(\langle v, v \rangle) \rightarrow \mathcal{I}(v) = \mathcal{F}(\langle v, v \rangle)$$

$$\mathbb{C}_2: \forall v. \neg C(\langle v, v \rangle) \rightarrow \mathcal{I}(v) = \perp$$

Propagation:

$$\mathbb{C}_3 \text{ (None Propagation):}$$

$$\forall e. \mathcal{P}(\perp, e) = \perp$$

$$\mathbb{C}_4 \text{ (Aggregate Propagation):}$$

$$\forall p_1, p_2, v.$$

$$\text{tail}(p_1) = \text{tail}(p_2) \rightarrow$$

$$\text{let } u := \text{tail}(p_1) \text{ in}$$

$$\mathcal{P}[\mathcal{R}(\mathcal{F}(p_1), \mathcal{F}(p_2)), \langle u, v \rangle] =$$

$$\mathcal{R}[\mathcal{F}(p_1 \cdot \langle u, v \rangle), \mathcal{F}(p_2 \cdot \langle u, v \rangle)]$$

$$\mathbb{C}_5 \text{ (Single Path):}$$

$$\forall p, e. \mathcal{P}(\mathcal{F}(p), e) = \mathcal{F}(p \cdot e)$$

Reduction:

$$\mathbb{C}_6 \text{ (Identity):}$$

$$\forall n. \mathcal{R}(n, \perp) = n$$

$$\mathbb{C}_7 \text{ (Commutativity):}$$

$$\forall n, n'. \mathcal{R}(n, n') = \mathcal{R}(n', n)$$

$$\mathbb{C}_8 \text{ (Associativity):}$$

$$\forall n, n', n''. \mathcal{R}(\mathcal{R}(n, n'), n'') = \mathcal{R}(n, \mathcal{R}(n', n''))$$

$$\mathbb{C}_9 \text{ (Idempotency):}$$

$$\forall n. \mathcal{R}(n, n) = n$$

Termination:

$$\mathbb{C}_{10}: \forall p. \mathcal{R}(\mathcal{F}(p), \mathcal{F}(\text{simple}(p))) = \mathcal{F}(\text{simple}(p))$$

Fig. 9. Correctness and termination conditions

result for the reduction. We capture this property as the condition \mathbb{C}_{10} in Fig. 9. The following theorem states that \mathbb{C}_{10} is sufficient for termination.

THEOREM 6 (TERMINATION). *For all \mathcal{R} , \mathcal{F} , and C , if the graph is acyclic or the condition \mathbb{C}_{10} holds, then there exists k such that for every $k' \geq k$, $\text{Spec}^{k'}(v) = \text{Spec}(v)$.*

Let l be the length of the longest simple path to the vertex v . After the iteration $k = l + 1$, the value of $\text{Spec}^k(v)$ stays unchanged. This is because the reduction over the paths of length greater than l does not change the value of $\text{Spec}^k(v)$. Any path p of length greater than l is not simple, i.e., it includes a cycle. This is refuted if the graph is acyclic. Otherwise, the simplification of p , $\text{simple}(p)$, is already in the set of paths of length less than $l + 1$ and by the condition \mathbb{C}_{10} , reducing the path value of p with the path value of $\text{simple}(p)$ results in the path value of $\text{simple}(p)$.

An immediate corollary of the above theorem is that if the graph is acyclic or the condition \mathbb{C}_{10} holds, then the above iteration models eventually terminate and converge to the specification (if the corresponding conditions in Theorem 2 to Theorem 5 hold). The final iteration is simply the maximum value of k from the above theorem for all vertices. For example, the corollary for the pull model for idempotent reduction functions is the following.

COROLLARY 7 (TERMINATION FOR PULL MODEL WITH IDEMPOTENT REDUCTION). *For all \mathcal{R} , \mathcal{F} , C , \mathcal{I} , and \mathcal{P} , if the conditions $\mathbb{C}_1 - \mathbb{C}_9$ hold, and the graph is acyclic or the condition \mathbb{C}_{10} holds, then there exists an iteration k such that $\mathcal{S}_{\text{pull}+}^k(v) = \text{Spec}(v)$.*

5.2 Synthesis of Iterative Reduction

In this subsection, we use the correctness conditions presented in the previous subsection to automatically synthesize correct-by-construction kernel functions.

Given a path-based reduction \mathcal{R} \mathcal{F} , the goal is to synthesize the kernel functions that are used by a target iterative reduction model. For example, consider the push iteration model with idempotent reduction that we saw in Def. 3. By Theorem 4, we need to find the functions \mathcal{I} , \mathcal{P}' and \mathcal{R}' such that the conditions $\mathbb{C}_1 - \mathbb{C}_{10}$ (presented in Fig. 9) hold. We use these conditions to synthesize the functions \mathcal{I} , \mathcal{P}' and \mathcal{R}' . In particular, (1) we use the initialization conditions $\mathbb{C}_1 - \mathbb{C}_2$ to synthesize \mathcal{I} . (2) We use the propagation condition \mathbb{C}_4 and \mathbb{C}_5 to synthesize \mathcal{P} and then wrap it in the following function \mathcal{P}' to handle none \perp values and satisfy the condition \mathbb{C}_3 .

$$\mathcal{P}' := \lambda n, e. \text{ if } (n = \perp) \text{ return } \perp \text{ else return } \mathcal{P}(n, e)$$

(3) We check the conditions $\mathbb{C}_7 - \mathbb{C}_9$ for the reduction function \mathcal{R} . Then, we wrap \mathcal{R} in the following reduction function \mathcal{R}' to handle none \perp values and satisfy the condition \mathbb{C}_6 .

$$\mathcal{R}' := \lambda a, b. \text{ if } (a = \perp) \text{ return } b \text{ else if } (b = \perp) \text{ return } a \\ \text{ else return } \mathcal{R}(a, b)$$

If the conditions $\mathbb{C}_7 - \mathbb{C}_9$ hold for \mathcal{R} , they hold for \mathcal{R}' as well.

To find candidate expressions for the body of the kernel functions, we apply a type-guided enumerative search. It enumerates expressions from the grammar that we saw in Fig. 4a in the order of increasing size. To support overloaded operators, the expression constructors have union types. To synthesize an expression of the given type, the search only considers expression constructors that return that type. It then recursively searches for the arguments and uses memoization to avoid redundant enumeration.

The procedure that synthesizes \mathcal{P} starts by memoizing expressions of size one, literals and variables, to make them available for the synthesis of the body of \mathcal{P} . Let T be the return type of \mathcal{F} ; vertices store values of type T . The propagation function \mathcal{P} takes a value stored at a vertex (of

type of T) and an edge (of type Edge) and returns a vertex value (of type T). Thus, the two input parameters of type T and Edge are memoized as available expressions. Then, candidate bodies for \mathcal{P} of type T of increasing sizes are incrementally obtained. A candidate propagation function $\lambda n, l. e$ is correct if the conditions \mathbb{C}_4 and \mathbb{C}_5 are valid when \mathcal{P} is replaced by the candidate. The context of the validity check $\mathcal{F}; \mathcal{R}; \Gamma$ is the definition of the functions \mathcal{F} and \mathcal{R} from the given path-based reduction, and a set of assertions Γ that define basic graph functions and relations. We model paths as lists of vertices and define graph functions and relations including the path functions length, weight, punultimate and capacity in the combination of the quantified uninterpreted functions and list theories. More details including the assertions Γ are available in the appendix § 3.2. The synthesis of the other kernel functions is similar.

For termination, we check a stronger condition than \mathbb{C}_{10} . Instead of removing cycles, we remove an edge: for every path p and edge e , if reducing the \mathcal{F} value of p with the \mathcal{F} value of $p \cdot e$ results in the former, then the reduction is terminating. (For synthesis in the push variant that requires rollback, after the propagation function is synthesized, a condition on the propagation \mathcal{P} and rollback \mathcal{B} functions is used to synthesize the rollback function (appendix § 3.1.2).)

6 EXPERIMENTAL RESULTS

Implementation. We implemented the GRAFS synthesis tool in three parts: fusion, synthesis and backends. The fusion phase closely follows the fusion rules (of § 4.2) using on the visitor pattern. The synthesis phase uses the Z3 SMT solver to check the validity of the correctness conditions. GRAFS incorporates a dedicated backend for each framework. Each backend generates a framework-specific C++ file containing the initialization \mathcal{I} , propagation \mathcal{P} , (if needed rollback \mathcal{B}) and reduction \mathcal{R} functions. (The different mappings for each of the target frameworks are presented in the appendix § 5.1.) GRAFS can be modularly extended with backends for new frameworks.

Platform and benchmarks. We performed the experiments on an 4-node cluster, each with 8 cores and 64GB memory. The experiments for frameworks that are exclusively for shared memory are performed on one of these nodes. The nodes are connected via 40Gbps InfiniBand network, and they run CentOS 7.4 Linux 3.10.0.x86_64. All programs are compiled with gcc-5.1.0 (for Ligra, Grid-Graph and GraphIt) and mpich-3.2.1 (for PowerGraph and Gemini). Fig. 10 lists the characteristics of the input datasets. We executed each experiment 5 times and reported the average.

Evaluation Summary. To evaluate the GRAFS synthesis tool, we compare the synthesized code with available handwritten versions in the frameworks. Experimental results show that the synthesized code either matches or outperforms handwritten code. We also study the effect of fusion on the performance of the generated code. Experimental results show that fusion can lead up to 4× faster execution time compared to the unfused baseline. We also report the synthesis time. GRAFS can efficiently generate programs in less than a minute.

Synthesized Matching Handwritten. We used five use-cases **BFS**, **CC**, **SSSP**, **WP** (widest path) and **PR** (page-rank) to compare the performance of the synthesized programs and their equivalent handwritten programs. We adopted the hand-written implementations of **BFS**, **CC**, **SSSP** and **PR** that are available in the frameworks, and developed **WP** based on **SSSP** by changing the path function. We ran **PR** on the input graphs until convergence. To thoroughly study the performance of the synthesized programs, we measure two metrics: the *number of edges processed* and the *execution time*. The *number of edges processed* by a program indicates how many times propagation happens across edges, and hence, the amount of computation performed throughout the execution. Since path-based calculations have asynchronous semantics [Vora 2017], vertex values can take

Dataset	V	E	Data
LiveJournal (LJ)	4.8M	68.9M	1.1G
twitter-www (TW)	41.6M	1.4B	23G
twitter-mpi (TM)	52.5M	1.9B	28G
Friendster (FR)	65.6M	1.8B	31G

Fig. 10. Dataset Characterization

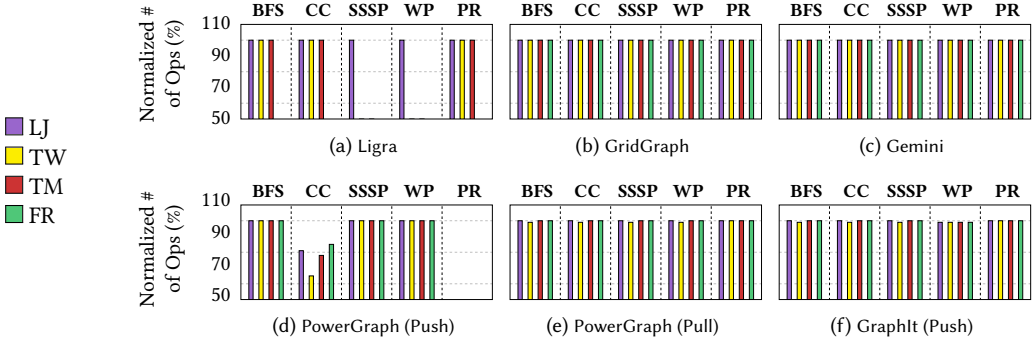


Fig. 11. Edge-work ratio: the normalized number of edges processed by the synthesized programs over the handwritten programs. The target for the five basic use-cases is 100%; lower ratios show further improvement. Missing bars are due to either missing handwritten use-cases (PR) or a timed-out after 24 hours.

Table 1. Execution times (in seconds). H: Handwritten, S: Synthesized, R: the ratio $\frac{H}{S}$. Missing cells are due to either missing handwritten use-cases (PR) or the corresponding experiment timed-out after 24 hours.

Prog.	Input	Ligra			GridGraph			Gemini			PowerGraph (Push)			PowerGraph (Pull)			GraphIt (Push)		
		H	S	R	H	S	R	H	S	R	H	S	R	H	S	R	H	S	R
BFS	LJ	3.28	3.17	1.03	1.56	1.56	1	0.25	0.26	0.96	6.1	6.4	0.95	11.6	11.2	1.04	0.39	.35	1.1
	TW	132	128	1.03	210	195	1.07	3.1	4.1	0.75	45.6	39	1.17	117.9	112.6	1.05	6	5.2	1.15
	TM	260	243	1.06	487	472	1.03	55	46	1.2	38.6	35.5	1.09	93.6	97	0.96	12.4	10.6	1.17
	FR	-	-	-	521	532	0.97	16	17.3	0.92	51.3	64.8	0.79	122.1	110.3	1.11	61	71.2	0.86
CC	LJ	1.69	1.78	0.94	2.21	2.22	0.99	0.79	0.81	1	13	11.7	1.11	22	19.1	1.15	0.48	0.4	1.15
	TW	131	120	1.09	230	214	1.07	7.3	7.7	0.94	97.6	66.4	1.47	167.3	157.4	1.06	10.6	10.6	1
	TM	184	187	0.98	432	423	1.02	16	19.5	0.82	128.8	95.5	1.35	219.4	196.3	1.12	316	351	0.9
	FR	-	-	-	606	599	1.01	51	48	1.06	223.9	184.3	1.21	375	353	1.06	26.6	22.8	1.16
SSSP	LJ	4.61	4.8	0.96	2.42	2.1	1.15	0.38	0.4	0.95	6.1	6.6	0.92	12.6	12.8	0.98	0.41	0.47	0.88
	TW	-	-	-	201	205	0.98	4.1	5	0.82	34.7	33.2	1.05	105.3	98.7	1.07	8.8	9.2	0.95
	TM	-	-	-	490	487	1	10	9.1	1.09	32	34.3	0.93	90.6	84.9	1.07	115.2	116.8	0.98
	FR	-	-	-	572	570	1	21	24	0.87	48.6	41.8	1.16	116	121.9	0.95	83	77.8	1.07
WP	LJ	6.53	6.4	1.02	3.46	3.2	1.08	0.43	0.41	1.04	5.7	5.8	0.98	10.7	10.5	1.02	0.49	0.44	1.11
	TW	-	-	-	245	242	1.01	4.3	4.8	0.9	35	34.8	1.01	110.5	105.7	1.05	9.8	8.8	1.11
	TM	-	-	-	479	498	0.96	9	7	1.2	34.4	31.4	1.10	94.2	81.9	1.15	4762	5212	0.9
	FR	-	-	-	551	545	1.01	26	24	1.08	47	46.4	1.01	109.1	102.3	1.07	169	165	1.01
PR	LJ	132	120	1	44	37	1.1	21	21	1	-	-	-	80	80	1	11.8	11.4	1.03
	TW	8290	8270	1.01	1000	908	1.1	282	400	0.7	-	-	-	1128	1041	1.08	319	331	0.96
	TM	13500	14700	0.91	1399	1441	0.97	880	860	1.02	-	-	-	1157	1078	1.07	596	613	0.97
	FR	-	-	-	1023	995	1.02	590	577	1.02	-	-	-	601	548	1.09	260	280	0.93

different execution paths before converging to the final results, resulting in different amount of edges processed for the same use-case. This means, a poorly synthesized program can perform redundant edge computations but can still converge to the correct result, and hence, we compare the number of edges processed by synthesized and handwritten programs. The second metric is the *execution time*. Although the execution time is primarily dependent on the number of processed edges, it is also dependent on the efficiency of the kernel functions which can be optimized by generating minimal vertex and edge variables and the minimal use of atomic operations.

Assessment. Fig. 11 shows the number of edges processed by the synthesized programs normalized w.r.t. that processed by the handwritten programs (i.e. the former divided by the latter), that we call edge-work ratio. We observe that the synthesized programs match or outperform handwritten programs. They process the same number of edges compared to handwritten programs in Ligra, GridGraph and Gemini. On PowerGraph and GraphIt, the synthesized programs process fewer edges. While the reduction is less than 1% in most cases, it is visible for the use-case **CC** in the push model and slightly visible for the TW input graph in the pull model and WP in the GraphIt. This

Table 2. Metrics for comparing handwritten and synthesized code. H: Handwritten, S: Synthesized. (PowerGraph does not require the user to write atomic operations and hence the last two columns are zeros.)

Prog.	Vertex Data Size (bytes) :: Edge Data Size (bytes)										# Atomics Per Edge									
	Ligra		GridGraph		Gemini		PowerGraph		GraphLT		Ligra		GridGraph		Gemini		PowerGraph		GraphLT	
	H	S	H	S	H	S	H	S	H	S	H	S	H	S	H	S	H	S	H	S
BFS	8::0	8::0	8::0	8::0	8::0	8::0	12::0	12::0	4::0	8::0	1	1	1	1	1	1	0	0	1	1
CC	4::0	4::0	4::0	4::0	4::0	4::0	8::0	8::0	4::0	4::0	1	1	1	1	1	1	0	0	1	1
SSSP	4::4	4::4	4::4	4::4	4::4	4::4	4::4	4::4	4::4	4::4	1	1	1	1	1	1	0	0	1	1
WP	4::4	4::4	4::4	4::4	4::4	4::4	4::4	4::4	4::4	4::4	1	1	1	1	1	1	0	0	1	1
PR	4::0	4::0	4::0	4::0	8::0	8::0	8::0	8::0	4::0	4::0	1	1	1	1	1	1	0	0	0	0

is because the synthesized programs initialize vertices by directly mapping over them, while the handwritten programs perform initialization in the apply step of the first iteration. Initialization in the apply step results in additional edge propagations in the first iteration. This has a high impact on the edge-work ratio for **CC** in the push model (down to 77%). Since all vertices need to be initialized in this use-case, the handwritten version unnecessarily processes all edges in the first iteration.

Table 1 shows the execution times of the handwritten programs (H), synthesized programs (S) and their relative ratio (R), i.e., former divided by the latter. We observe that the execution time is closely related to the number of processed edges (**Fig. 11**). The performance of the handwritten and synthesized code is similar in most cases. The synthesized **CC** for PowerGraph in the push model, performs 28% faster in average.

Running the same program (either synthesized or handwritten) multiple times shows a variance in the execution time due to variances from the runtime environment. To have a more precise comparison, we further compare the number of atomic operations per edge computation, and the size of state maintained per vertex and edge, which are two major sources of inefficiency in graph computations. The results are shown in **Table 2**. The number of atomic operations per edge, the size of vertex, and edge states are equal in synthesized and handwritten programs.

Fusion Types. In order to study the performance benefits of the different fusion types that the fusion rules represent, we compare the unfused and the fused implementations of three representative use-cases **WSP**, **NWR** and **RADIUS** (presented in **Fig. 1**). **Fig. 13** shows the number of edges processed by the synthesized (fused) programs normalized w.r.t. that by the unfused versions, that we call edge-work ratio. We visit the use-cases and the applied fusion rules (from § 4.2) in turn.

WSP. **WSP** is fused by the rule **FPNEST**. As described earlier in § 4.2, this rule fuses nested path-based reductions. The unfused program for this use-case consists of two computation phases over the edges of the input graph, one after the other. The first phase calculates the shortest paths from the given source to all the vertices, and the second phase computes the capacity of the widest path across the shortest paths. The fused program, however, executes the two computations in one pass over a pair of values.

Assessment. **Fig. 13a** (for unweighted graphs) and **Fig. 13d** (for weighted graphs) show the edge-work ratio for **WSP**. In unweighted graphs, the fused program processes half the number of edges processed by the unfused program. Similarly, on weighted graphs, the fused program processes 50-70% of the edges processed by the unfused program. When graphs are unweighted, each edge represents a unit cost (that can be either weight or capacity). In each iteration, the set of edges that contribute to the weight and capacity values of a vertex are the same. Hence, the fused program exploits this overlap by simultaneously propagating the two values across each edge; which reduces passes over the edges by 50%. However, for weighted graphs, the two values can be propagated to the vertex in different iterations since the min and max reductions result in different paths based on different edge weights. Hence, the processing of edges only partially overlap.

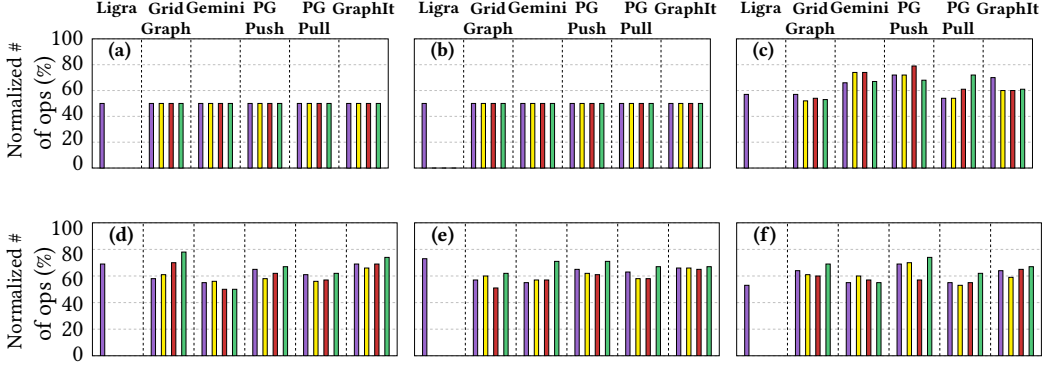


Fig. 13. Edge-work ratio: normalized # of edges processed by the fused version over the unfused version in unweighted graphs (a, b, c) and weighted graphs (d, e, f). (a) and (d) show WSP. (b) and (e) show NWR. (c) and (f) show RADIUS.

NWR. The unfused version of **NWR** calculates the narrowest and the widest paths separately. The two are fused by the rule **FMPAIR**. This rule fuses multiple path-based reductions into a single path-based reduction; it translates the reduction functions to a single reduction function that operates on pairs.

Assessment. Fig. 13b (for unweighted graphs) and Fig. 13e (for weighted graphs) show the edge-work ratio for **NWR**. Similar to **WSP**, the fused program reduces the number of processed edges by 50% for unweighted graphs and by 51-73% for weighted graphs. The fused version propagates the narrowest and widest values over an edge at the same time. Thus, it benefits from both overlapping propagations and locality of the memory accesses.

RADIUS. **RADIUS** is fused by the rule **FMPAIR** that we considered above and the rule **FRPAIR**. The rule **FRPAIR** fuses multiple vertex-based reductions into a single reduction. **RADIUS** computes eccentricity (i.e. the maximum shortest distance) by sampling a set of sources. We sample two source vertices. The unfused version computes eccentricity separately for each source. However, the rules **FMPAIR** and **FRPAIR** fuse the path-based and vertex-based reductions across the sources to a single path-based and a single vertex-based reduction.

Assessment. Fig. 13c (for unweighted graphs) and Fig. 13f (for weighted graphs) show the edge-work ratio for **RADIUS**. We observe that on unweighted graphs, the fused version processes 52-78% of the number of edges that the unfused version processes. This ratio is 53-74% on weighted graphs. Even though fusion enables computation of multiple eccentricity values at the same time, contrary to **WSP** and **NWR**, we do not observe the 50% reduction. This is because eccentricity computations across different sources can occur via paths that don't necessarily overlap. The fused version exploits the partial overlaps.

We observe that the reduction in edge computations is different across different frameworks as well. For example, the edge-work ratio is 52-68% in GridGraph, whereas 54-78% in PowerGraph. This is because of the difference in the scheduling strategies across these different frameworks, that lead to different overlaps in edge computations. This means that even if the same edge propagates values for multiple sources, certain frameworks may schedule processing of that edge for different sources in different iterations.

Next, we consider the edge-work ratio and absolute execution times for more elaborate use-cases with multiple fusions. (Due to space limitation, the absolute execution times for the simpler use-cases above, **WSP**, **NWR** and **RADIUS**, are available in the appendix § 6.2. Further, more experiments

Table 3. Execution times (in seconds). H: Handwritten, S: Synthesized, R: the ratio $\frac{H}{S}$.

Prog.	Input	Ligra			GridGraph			Gemini			PowerGraph (Push)			PowerGraph (Pull)			GraphIt (Push)		
		H	S	R	H	S	R	H	S	R	H	S	R	H	S	R	H	S	R
DRR	LJ	13.1	4	3.2	15.3	3.8	4	0.9	0.3	3	20.4	6.4	3.2	36	10	3.6	0.35	1	2.8
	TW	-	-	-	82	23	3.6	11.1	5.5	2	120	48	2.5	292	81	3.6	6.7	20.7	3
	TM	-	-	-	141	44	3.3	18.2	6.3	2.9	166	50	3.3	462	86	2.9	12.2	34.7	3.5
	FR	-	-	-	265	73	3.6	36	17	2	247	86	2.9	522	154	3.4	17	47	3.5
Trust	LJ	12.3	6	2.05	14.1	4.4	3.2	0.76	0.37	2	20.5	7.5	2.7	37	10	3.7	0.47	1	2.2
	TW	-	-	-	85	28	3.1	10.5	6.6	1.6	122	50	2.4	293	99	2.9	11.7	22	2
	TM	-	-	-	122	40	3	14.5	8	1.8	157	71	2.2	455	129	3.5	23.3	80	3.4
	FR	-	-	-	218	117	2	34.5	16	2.2	252	98	2.6	526	173	3	25	52	2
RDS	LJ	14.4	7.8	1.8	11.5	6	1.9	0.9	0.6	1.5	23	15.1	1.5	41	28	1.4	0.73	1	1.4
	TW	-	-	-	74	47	1.6	11	6	1.8	130	108	1.2	-	-	-	13.2	20.5	1.5
	TM	-	-	-	142	82	1.7	11	7.8	1.4	200	134	1.5	-	-	-	23	45.7	2
	FR	-	-	-	210	175	1.2	37	19	1.9	286	198	1.5	-	-	-	19	35	1.7

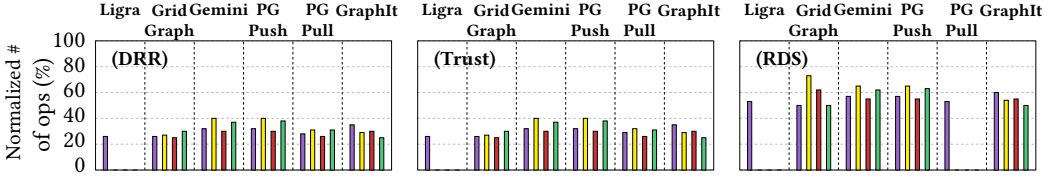


Fig. 14. Edge-work ratio: Normalized # of edges processed by the fused version over the unfused version.

including the scalability of the fusion process on increasing number of sources in the **RADIUS** use-case are available in the appendix § 6.1.)

Multiple Fusions. We study the performance benefits of fusion on more elaborated use-cases: **TRUST**, **DRR**, and **RDS** (presented in Fig. 1). We report both edge-work ratio and absolute execution times in Fig. 14 and Table 3 respectively. Our experimental results show that fusion reduces the edge-work ratio to a quarter and leads to up-to 4× speedup.

DRR. **DRR** calculates the ratio of the diameter over radius sampled over two sources. In addition to the rules **FMPAIR**, **FRPAIR** and **FLETsBIN** which fuse path-based and vertex-based reductions, common operation elimination rules (the appendix § 2.2.1) eliminate redundant path-based computations in diameter and radius. Therefore, instead of 4 reductions, GRAFS fuses and calculates 1 reduction (appendix § 2.3). In Fig. 14, we observe that the edge-work ratio is 25-40%. This translates to 2-4× speedup in Table 3. Note that the theoretical bound on the edge-work ratio is 25%, which is achieved when the path-based computations for the two sources fully overlap.

TRUST. **TRUST** specifies the trust from a given set of nodes to other nodes. It applies division and maximum operators between path-based reductions: the widest and shortest paths. The rules **FILETBin** and **FMPAIR** fuse the 4 path-based reductions to 1. As shown in Fig. 14, the edge-work ratio is 25-40%, and Table 3 shows, the speedup across different frameworks is 1.6-3.7×. The theoretical bound on the edge-work ratio is again 25%, similar to the **DRR** use-case.

RDS. Given a source s , **RDS** calculates the narrowest of the widest paths to vertices within the radius neighbourhood of s . **RDS** has a nested reduction for **RADIUS** and is transformed by fusion rules for nested vertex-based reductions (appendix § 2.2.6). The inner **RADIUS** is factored and fused as before. Moreover, the two path-based reductions, the narrowest and shortest paths, are fused by the rules **FILETBin** and **FMPAIR**. This results in a sequence of two iteration-map-reduce rounds. The theoretical bound for the edge-work ratio is 50% mainly because the fused and unfused programs perform two and four sequences of iteration-map-reduce rounds respectively. Fig. 14 shows that the edge-work ratio is 57-85% which translates to 1.2-2× speedup in Table 3.

Synthesis time. Fig. 15 presents the synthesis time that is below 2 minutes and often seconds. The use cases that require desugaring (**BFS**) or fusion of nested reductions (**WSP**) take more time.

7 RELATED WORK

Graph Processing Frameworks and Synthesis. Graph processing systems provide interfaces to hide the implementation details such as parallelism, synchronization and communication in scalable runtimes. At the heart of graph computations are operations over vertex and edge values and scheduling policies to determine the order in which operations are performed. Parallelism is often extracted at the vertex and edge level, and hence, most interfaces allow computations to be directly expressed as vertex-level and edge-level operations [Dathathri et al. 2018; Gonzalez et al. 2012; Grossman et al. 2018; Hoang et al. 2019; Low et al. 2012, 2014; Malewicz et al. 2010; Nguyen et al. 2013; Roy et al. 2013; Shun and Blelloch 2013; Zhang et al. 2018; Zhu et al. 2016, 2015]. Certain DSLs raise the level of abstraction in order to simplify development of graph algorithms [Aberger et al. 2017; Hong et al. 2012; Rodriguez 2015; Sevenich et al. 2016; van Rest et al. 2016]. Contrary to our synthesis process, graph processing DSLs [Cheramangalath et al. 2017; Emoto et al. 2016; Gill et al. 2018; Shashidhar and Nasre 2016] require users to write vertex- or edge-level kernel functions. However, they provide implementations for different architectures such as GPUs and distributed platforms. Further, they generate implementations that are tied to their runtime specifics. In the synthesis domain, Elixir [Prountzos et al. 2012, 2015] synthesizes multiple parallel implementations from the specification of a graph computation and applies automated reasoning to optimize them. In contrast, GRAFS offers a more high-level specification language and automatically synthesizes the kernel functions.

Program Synthesis. Program synthesis has always been an area of interest for computer scientists. Previous works have employed enumeration [Itzhaky et al. 2010; Udupa et al. 2013], variants of syntax-guided synthesis [Alur et al. 2013] and type-guided synthesis [Osera and Zdancewic 2015; Polikarpova et al. 2016] to synthesize protocol snippets [Udupa et al. 2013] and Excel macros [Gulwani 2011; Gulwani et al. 2012]. GRAFS’s synthesis process enumerates graph processing kernel functions based on a syntax grammar for local computations. Previous works have also used constraint solving to fill holes in program sketches [Solar-Lezama et al. 2005, 2006] including architectural kernel functions [Xu et al. 2014], and to synthesize control structures, imperative programs [Feng et al. 2017; Srivastava et al. 2010] and program templates [Barman et al. 2015] or to compose APIs [Jha et al. 2010; Shi et al. 2019]. The GRAFS synthesis tool applies SMT solvers to check that the candidate kernel functions satisfy the correctness conditions of the iterative models. Built on top of Fregel, [Morihata et al. 2018] uses SAT solvers to optimize kernel functions. In contrast, GRAFS automatically synthesizes the kernel functions. Superoptimization is another thread of synthesis which applies stochastic search methods to synthesize programs [Bansal and Aiken 2006; Joshi et al. 2002, 2006; Massalin 1987; Schkufza et al. 2013]. Moreover, Souper [Sasnauskas et al. 2017] took a step further by synthesizing superoptimizers. In contrary to superoptimization which focuses on optimizing machine-level code, GRAFS fusion rules optimize high-level graph processing specifications. Program synthesis has been also utilized to synthesize distributed programs [Houshmand and Lesani 2019; Smith and Albarghouthi 2016; Udupa et al. 2013].

Fusion. Fusion is a versatile optimization technique. Loop fusion [Bondhugula et al. 2008; Darte 1999; Kennedy and McKinley 1993; Qasem and Kennedy 2006] merges the bodies of loops on regular structures such as arrays and hence reduces the number of memory accesses and improves locality. Fusion also has been applied to tree structures [Rajbhandari et al. 2016a,b; Sakka et al.

Program	#PBR ¹	F ²	CS ³
BFS	1	51	25
CC	1	3	1
SSSP	1	2	24
WP	1	2	29
PR	-	-	-
WSP	2	93	44
NWR	2	2	58
RADIUS	2	2	49
DS	2	2	49
DRR	4	3	50
TRUST	4	3	105
RDS	4	10	102

¹ # of path-based reductions

² Fusion time (ms)

³ Constraint solving time (s)

Fig. 15. Analysis Time

2017, 2019] to combine multiple phases of traversal or fuse different stages of data processing pipelines [Saarikivi et al. 2017] to enhance data locality. Deforestation of functional programs [Chin 1992; Gill et al. 1993; Wadler 1988] combines a sequence of function applications into a single function application and eliminates intermediate values. However, deforestation is oblivious to the primitives of graph computation. Graph computations use three fundamental primitives; thus, we structure these primitives as the triple-let term. The fusion rules transform the computations to this structure and maintain it during fusion.

8 CONCLUSION

We saw GRAFS, a graph analytics language and synthesizer. It features semantics-preserving fusion optimizations. It automatically synthesizes kernel functions based on correctness conditions for iterative reductions. It generates code for high-performance graph processing frameworks. We hope that it motivates further research to simplify and accelerate data analytics.

REFERENCES

- Christopher R Aberger, Andrew Lamb, Susan Tu, Andres Nötzli, Kunle Olukotun, and Christopher Ré. 2017. Emptyheaded: A relational engine for graph processing. *ACM Transactions on Database Systems (TODS)* 42, 4 (2017), 20.
- Rajeev Alur, Rastislav Bodik, Garvit Juniwal, Milo MK Martin, Mukund Raghothaman, Sanjit A Seshia, Rishabh Singh, Armando Solar-Lezama, Emina Torlak, and Abhishek Udupa. 2013. Syntax-guided synthesis. In *2013 Formal Methods in Computer-Aided Design*. IEEE, 1–8.
- Appendix. 2019. *Submitted Supplement Document*.
- Sorav Bansal and Alex Aiken. 2006. Automatic generation of peephole superoptimizers. In *ACM Sigplan Notices*, Vol. 41. ACM, 394–403.
- Shaon Barman, Rastislav Bodik, Satish Chandra, Emina Torlak, Arka Bhattacharya, and David Culler. 2015. Toward tool support for interactive synthesis. In *2015 ACM International Symposium on New Ideas, New Paradigms, and Reflections on Programming and Software (Onward!)*. ACM, 121–136.
- Uday Bondhugula, Albert Hartono, J. Ramanujam, and P. Sadayappan. 2008. A Practical Automatic Polyhedral Parallelizer and Locality Optimizer. In *Proceedings of the 29th ACM SIGPLAN Conference on Programming Language Design and Implementation (PLDI '08)*. ACM, New York, NY, USA, 101–113. <https://doi.org/10.1145/1375581.1375595>
- Unnikrishnan Cheramangalath, Rupesh Nasre, and Y N. Srikant. 2017. DH-Falcon: A Language for Large-Scale Graph Processing on Distributed Heterogeneous Systems. 439–450. <https://doi.org/10.1109/CLUSTER.2017.72>
- Wei-Ngan Chin. 1992. Safe fusion of functional expressions. In *ACM SIGPLAN Lisp Pointers*. ACM, 11–20.
- Alain Darté. 1999. On the complexity of loop fusion. In *1999 International Conference on Parallel Architectures and Compilation Techniques (Cat. No. PR00425)*. IEEE, 149–157.
- Roshan Dathathri, Gurbinder Gill, Loc Hoang, Hoang-Vu Dang, Alex Brooks, Nikoli Dryden, Marc Snir, and Keshav Pingali. 2018. Gluon: A Communication-optimizing Substrate for Distributed Heterogeneous Graph Analytics. In *Proceedings of the 39th ACM SIGPLAN Conference on Programming Language Design and Implementation (PLDI 2018)*. ACM, New York, NY, USA, 752–768. <https://doi.org/10.1145/3192366.3192404>
- Kento Emoto, Kiminori Matsuzaki, Zhenjiang Hu, Akimasa Morihata, and Hideya Iwasaki. 2016. Think like a vertex, behave like a function! a functional DSL for vertex-centric big graph processing. *ACM SIGPLAN Notices* 51 (09 2016), 200–213. <https://doi.org/10.1145/3022670.2951938>
- Yu Feng, Ruben Martins, Yuepeng Wang, Isil Dillig, and Thomas W Reps. 2017. Component-based synthesis for complex APIs. *ACM SIGPLAN Notices* 52, 1 (2017), 599–612.
- Andrew Gill, John Launchbury, and Simon L. Peyton Jones. 1993. A Short Cut to Deforestation. In *Proceedings of the Conference on Functional Programming Languages and Computer Architecture (FPCA '93)*. ACM, New York, NY, USA, 223–232. <https://doi.org/10.1145/165180.165214>
- Gurbinder Gill, Roshan Dathathri, Loc Hoang, Andrew Lenharth, and Keshav Pingali. 2018. Abelian: A Compiler for Graph Analytics on Distributed, Heterogeneous Platforms. In *Euro-Par 2018: Parallel Processing*, Marco Aldinucci, Luca Padovani, and Massimo Torquati (Eds.). Springer International Publishing, Cham, 249–264.
- Jennifer Ann Golbeck. 2005. *Computing and applying trust in web-based social networks*. Ph.D. Dissertation.
- Joseph E Gonzalez, Yucheng Low, Haijie Gu, Danny Bickson, and Carlos Guestrin. 2012. Powergraph: Distributed graph-parallel computation on natural graphs. In *Presented as part of the 10th {USENIX} Symposium on Operating Systems Design and Implementation ({OSDI} 12)*. 17–30.

- Samuel Grossman, Heiner Litz, and Christos Kozyrakis. 2018. Making pull-based graph processing performant. In *ACM SIGPLAN Notices*, Vol. 53. ACM, 246–260.
- Sumit Gulwani. 2011. Automating string processing in spreadsheets using input-output examples. In *ACM SIGPLAN Notices*, Vol. 46. ACM, 317–330.
- Sumit Gulwani, William R Harris, and Rishabh Singh. 2012. Spreadsheet data manipulation using examples. *Commun. ACM* 55, 8 (2012), 97–105.
- Loc Hoang, Matteo Pontecorvi, Roshan Dathathri, Gurbinder Gill, Bozhi You, Keshav Pingali, and Vijaya Ramachandran. 2019. A round-efficient distributed betweenness centrality algorithm. In *Proceedings of the 24th Symposium on Principles and Practice of Parallel Programming*. 272–286.
- Sungpack Hong, Hassan Chafi, Edic Sedlar, and Kunle Olukotun. 2012. Green-Marl: a DSL for easy and efficient graph analysis. *ACM SIGARCH Computer Architecture News* 40, 1 (2012), 349–362.
- Farzin Houshmand and Mohsen Lesani. 2019. Hamsaz: replication coordination analysis and synthesis. *Proceedings of the ACM on Programming Languages* 3, POPL (2019), 74.
- Shachar Itzhaky, Sumit Gulwani, Neil Immerman, and Mooly Sagiv. 2010. A simple inductive synthesis methodology and its applications. In *ACM Sigplan Notices*, Vol. 45. ACM, 36–46.
- Susmit Jha, Sumit Gulwani, Sanjit A Seshia, and Ashish Tiwari. 2010. Oracle-guided component-based program synthesis. In *Proceedings of the 32nd ACM/IEEE International Conference on Software Engineering-Volume 1*. ACM, 215–224.
- Rajeev Joshi, Greg Nelson, and Keith Randall. 2002. Denali: a goal-directed superoptimizer. Vol. 37. ACM.
- Rajeev Joshi, Greg Nelson, and Yunhong Zhou. 2006. Denali: A practical algorithm for generating optimal code. *ACM Transactions on Programming Languages and Systems (TOPLAS)* 28, 6 (2006), 967–989.
- Ken Kennedy and Kathryn S McKinley. 1993. Maximizing loop parallelism and improving data locality via loop fusion and distribution. In *International Workshop on Languages and Compilers for Parallel Computing*. Springer, 301–320.
- Yucheng Low, Danny Bickson, Joseph Gonzalez, Carlos Guestrin, Aapo Kyrola, and Joseph M Hellerstein. 2012. Distributed GraphLab: a framework for machine learning and data mining in the cloud. *Proceedings of the VLDB Endowment* 5, 8 (2012), 716–727.
- Yucheng Low, Joseph E Gonzalez, Aapo Kyrola, Danny Bickson, Carlos E Guestrin, and Joseph Hellerstein. 2014. Graphlab: A new framework for parallel machine learning. *arXiv preprint arXiv:1408.2041* (2014).
- Grzegorz Malewicz, Matthew H Austern, Aart JC Bik, James C Dehnert, Ilan Horn, Naty Leiser, and Grzegorz Czajkowski. 2010. Pregel: a system for large-scale graph processing. In *Proceedings of the 2010 ACM SIGMOD International Conference on Management of data*. ACM, 135–146.
- Harry Massalin. 1987. Superoptimizer – a Look at the Smallest Program. *Palo Alto, California* (1987).
- Akimasa Morihata, Kento Emoto, Kiminori Matsuzaki, Zhenjiang Hu, and Hideya Iwasaki. 2018. Optimizing Declarative Parallel Distributed Graph Processing by Using Constraint Solvers. In *Functional and Logic Programming*, John P. Gallagher and Martin Sulzmann (Eds.). Springer International Publishing, Cham, 166–181.
- Donald Nguyen, Andrew Lenharth, and Keshav Pingali. 2013. A lightweight infrastructure for graph analytics. In *Proceedings of the Twenty-Fourth ACM Symposium on Operating Systems Principles*. ACM, 456–471.
- Peter-Michael Osera and Steve Zdancewic. 2015. Type-and-example-directed program synthesis. *ACM SIGPLAN Notices* 50, 6 (2015), 619–630.
- Nadia Polikarpova, Ivan Kuraj, and Armando Solar-Lezama. 2016. Program synthesis from polymorphic refinement types. In *ACM SIGPLAN Notices*, Vol. 51. ACM, 522–538.
- Dimitrios Proutzos, Roman Manevich, and Keshav Pingali. 2012. Elixir: A system for synthesizing concurrent graph programs. In *ACM SIGPLAN Notices*, Vol. 47. ACM, 375–394.
- Dimitrios Proutzos, Roman Manevich, and Keshav Pingali. 2015. Synthesizing parallel graph programs via automated planning. In *ACM SIGPLAN Notices*, Vol. 50. ACM, 533–544.
- Apan Qasem and Ken Kennedy. 2006. Profitable Loop Fusion and Tiling Using Model-driven Empirical Search. In *Proceedings of the 20th Annual International Conference on Supercomputing (ICS '06)*. ACM, New York, NY, USA, 249–258. <https://doi.org/10.1145/1183401.1183437>
- Samyam Rajbhandari, Jinsung Kim, Sriram Krishnamoorthy, Louis-Noel Pouchet, Fabrice Rastello, Robert J Harrison, and Ponnuswamy Sadayappan. 2016a. A domain-specific compiler for a parallel multiresolution adaptive numerical simulation environment. In *Proceedings of the International Conference for High Performance Computing, Networking, Storage and Analysis*. IEEE Press, 40.
- Samyam Rajbhandari, Jinsung Kim, Sriram Krishnamoorthy, Louis-Noël Pouchet, Fabrice Rastello, Robert J Harrison, and Ponnuswamy Sadayappan. 2016b. On fusing recursive traversals of Kd trees. In *Proceedings of the 25th International Conference on Compiler Construction*. ACM, 152–162.
- Marko A Rodriguez. 2015. The gremlin graph traversal machine and language (invited talk). In *Proceedings of the 15th Symposium on Database Programming Languages*. ACM, 1–10.

- Amitabha Roy, Ivo Mihailovic, and Willy Zwaenepoel. 2013. X-stream: Edge-centric graph processing using streaming partitions. In *Proceedings of the Twenty-Fourth ACM Symposium on Operating Systems Principles*. ACM, 472–488.
- Olli Saarikivi, Margus Veanes, Todd Mytkowicz, and Madan Musuvathi. 2017. Fusing Effectful Comprehensions. *SIGPLAN Not.* 52, 6 (June 2017), 17–32. <https://doi.org/10.1145/3140587.3062362>
- Laith Sakka, Kirshanthan Sundararajah, and Milind Kulkarni. 2017. Treefuser: a framework for analyzing and fusing general recursive tree traversals. *Proceedings of the ACM on Programming Languages* 1, OOPSLA (2017), 76.
- Laith Sakka, Kirshanthan Sundararajah, Ryan R Newton, and Milind Kulkarni. 2019. Sound, fine-grained traversal fusion for heterogeneous trees. In *Proceedings of the 40th ACM SIGPLAN Conference on Programming Language Design and Implementation*. ACM, 830–844.
- Raimondas Sasnauskas, Yang Chen, Peter Collingbourne, Jeroen Ketema, Gratian Lup, Jubi Taneja, and John Regehr. 2017. Souper: A synthesizing superoptimizer. *arXiv preprint arXiv:1711.04422* (2017).
- Eric Schkufza, Rahul Sharma, and Alex Aiken. 2013. Stochastic superoptimization. In *ACM SIGPLAN Notices*, Vol. 48. ACM, 305–316.
- Martin Sevenich, Sungpack Hong, Oskar van Rest, Zhe Wu, Jayanta Banerjee, and Hassan Chafi. 2016. Using domain-specific languages for analytic graph databases. *Proceedings of the VLDB Endowment* 9, 13 (2016), 1257–1268.
- G Shashidhar and Rupesh Nasre. 2016. Lighthouse: An automatic code generator for graph algorithms on gpus. In *International Workshop on Languages and Compilers for Parallel Computing*. Springer, 235–249.
- Kensen Shi, Jacob Steinhardt, and Percy Liang. 2019. FrAngel: Component-based Synthesis with Control Structures. *Proc. ACM Program. Lang.* 3, POPL, Article 73 (Jan. 2019), 29 pages. <https://doi.org/10.1145/3290386>
- Julian Shun and Guy E. Blelloch. 2013. Ligma: A Lightweight Graph Processing Framework for Shared Memory. In *Proceedings of the 18th ACM SIGPLAN Symposium on Principles and Practice of Parallel Programming (PPoPP '13)*. ACM, New York, NY, USA, 135–146. <https://doi.org/10.1145/2442516.2442530>
- Calvin Smith and Aws Albarghouthi. 2016. MapReduce program synthesis. *ACM SIGPLAN Notices* 51, 6 (2016), 326–340.
- Armando Solar-Lezama, Rodric Rabbah, Rastislav Bodik, and Kemal Ebcioglu. 2005. Programming by sketching for bit-streaming programs. In *ACM SIGPLAN Notices*, Vol. 40. ACM, 281–294.
- Armando Solar-Lezama, Liviu Tancau, Rastislav Bodik, Sanjit Seshia, and Vijay Saraswat. 2006. Combinatorial sketching for finite programs. *ACM Sigplan Notices* 41, 11 (2006), 404–415.
- Saurabh Srivastava, Sumit Gulwani, and Jeffrey S Foster. 2010. From program verification to program synthesis. In *ACM Sigplan Notices*, Vol. 45. ACM, 313–326.
- Abhishek Udupa, Arun Raghavan, Jyotirmoy V Deshmukh, Sela Mador-Haim, Milo MK Martin, and Rajeev Alur. 2013. TRANSIT: specifying protocols with concolic snippets. *ACM SIGPLAN Notices* 48, 6 (2013), 287–296.
- Oskar van Rest, Sungpack Hong, Jinha Kim, Xuming Meng, and Hassan Chafi. 2016. PGQL: a property graph query language. In *Proceedings of the Fourth International Workshop on Graph Data Management Experiences and Systems*. ACM, 7.
- Keval Vora. 2017. *Exploiting Asynchrony for Performance and Fault Tolerance in Distributed Graph Processing*. Ph.D. Dissertation. University of California, Riverside.
- Philip Wadler. 1988. Deforestation: Transforming Programs to Eliminate Trees. In *Proceedings of the Second European Symposium on Programming*. North-Holland Publishing Co., Amsterdam, The Netherlands, The Netherlands, 231–248. <http://dl.acm.org/citation.cfm?id=80098.80104>
- Zhilei Xu, Shoaib Kamil, and Armando Solar-Lezama. 2014. MSL: A Synthesis Enabled Language for Distributed Implementations. In *Proceedings of the International Conference for High Performance Computing, Networking, Storage and Analysis (SC '14)*. IEEE Press, Piscataway, NJ, USA, 311–322. <https://doi.org/10.1109/SC.2014.31>
- Yunming Zhang, Mengjiao Yang, Riyadh Baghdadi, Shoaib Kamil, Julian Shun, and Saman Amarasinghe. 2018. GraphIt: A High-performance Graph DSL. *Proc. ACM Program. Lang.* 2, OOPSLA, Article 121 (Oct. 2018), 30 pages. <https://doi.org/10.1145/3276491>
- Xiaowei Zhu, Wenguang Chen, Weimin Zheng, and Xiaosong Ma. 2016. Gemini: A computation-centric distributed graph processing system. In *12th {USENIX} Symposium on Operating Systems Design and Implementation ({OSDI} 16)*. 301–316.
- Xiaowei Zhu, Wentao Han, and Wenguang Chen. 2015. Gridgraph: Large-scale graph processing on a single machine using 2-level hierarchical partitioning. In *2015 {USENIX} Annual Technical Conference ({USENIX} {ATC} 15)*. 375–386.